Volume 15
Number 5
7 February 2024
Pages 1523–1908

Chemical Science

rsc.li/chemical-science

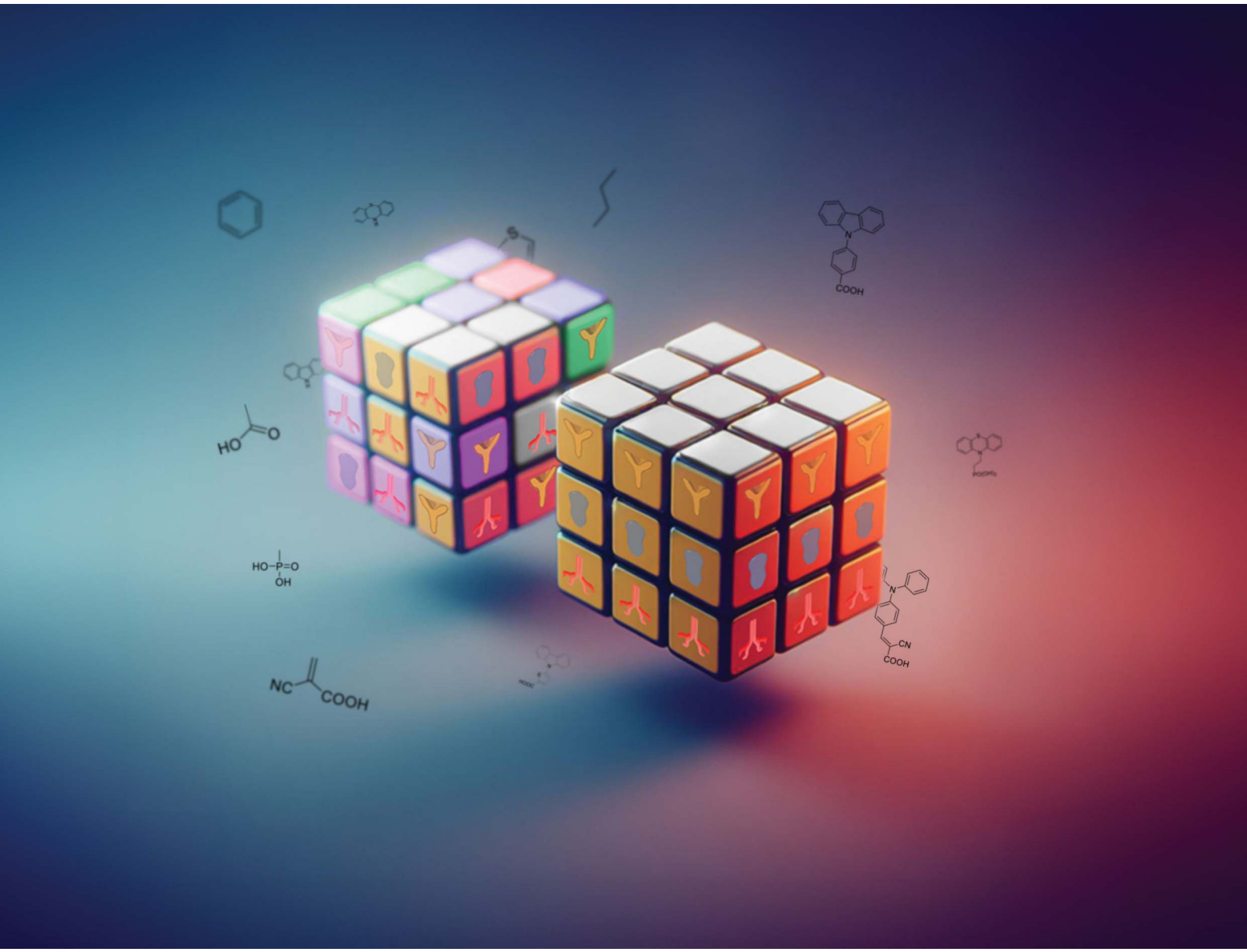

ISSN 2041-6539

ROYAL SOCIETY OF CHEMISTRY

PERSPECTIVE
Carlos E. Puerto Galvis, Emilio Palomares *et al.*
Challenges in the design and synthesis of self-assembling molecules as selective contacts in perovskite solar cells

Chemical Science

ROYAL SOCIETY OF CHEMISTRY

PERSPECTIVE

View Article Online
View Journal | View Issue

Check for updates

Cite this: *Chem. Sci.*, 2024, **15**, 1534

All publication charges for this article have been paid for by the Royal Society of Chemistry

Challenges in the design and synthesis of self-assembling molecules as selective contacts in perovskite solar cells

Carlos E. Puerto Galvis, *[a] Dora A. González Ruiz, [ab] Eugenia Martínez-Ferrero [a] and Emilio Palomares *[ac]

Self-assembling molecules (SAMs), as selective contacts, play an important role in perovskite solar cells (PSCs), determining the performance and stability of these photovoltaic devices. These materials offer many advantages over other traditional materials used as hole-selective contacts, as they can be easily deposited on a large area of metal oxides, can modify the work function of these substrates, and reduce optical and electric losses with low material consumption. However, the most interesting thing about SAMs is that by modifying the chemical structure of the small molecules used, the energy levels, molecular dipoles, and surface properties of this assembled monolayer can be modulated to fine-tune the desired interactions between the substrate and the active layer. Due to the important role of organic chemistry in the field of photovoltaics, in this review, we will cover the current challenges for the design and synthesis of SAMs PSCs. Discussing, the structural features that define a SAM, (ii) disclosing how commercial molecules inspired the synthesis of new SAMs; and (iii) detailing the pros- and cons- of the reported synthetic protocols that have been employed for the synthesis of molecules for SAMs, helping synthetic chemists to develop novel structures and promoting the fast industrialization of PSCs.

Received 4th September 2023
Accepted 8th November 2023

DOI: 10.1039/d3sc04668k

rsc.li/chemical-science

[a]*Institute of Chemical Research of Catalonia (ICIQ), Avda. Països Catalans, 16, Tarragona, Spain. E-mail: epalomares@iciq.es*
[b]*Departament d'Enginyeria Electrònica, Elèctrica i Automàtica., Universitat Rovira i Virgili, Avda. Països Catalans, 26, Tarragona, Spain*
[c]*Catalan Institution for Research and Advanced Studies (ICREA), Passeig Lluïs Companys, 23, Barcelona, Spain*

Introduction

Since their discovery in 2009, perovskite solar cells (PSCs) are considered nowadays amongst the most promising next-generation photovoltaic technologies.[1] PSCs have achieved

Carlos E. Puerto Galvis

Carlos E. Puerto Galvis received his PhD from the Universidad Industrial de Santander (Colombia) under the supervision of Prof. Vladimir Kouznetsov (2018). He is currently a postdoctoral researcher at the Institute of Chemical Research of Catalonia (Spain) under the supervision of Prof. Emilio Palomares. In 2019 he received the Young Colombian Scientists award by the Colombian Academy of Exact, Physical and Natural Sciences for his contributions to the field of organic chemistry. His current research interests include green chemistry, electrosynthesis, metal-free and organometallic C–H activation, C–C and C–N couplings for the synthesis of small molecules for medicinal chemistry and materials science.

Dora A. González Ruiz

Dora A. Gonzalez Ruiz obtained her M.Sc. in Chemistry at the Centre of Exact Sciences and Engineering (CUCEI), of the University of Guadalajara (Mexico). She is currently a PhD candidate in the group of Prof. Palomares at ICIQ since 2018, In 2021 she made a research stay at the School of Materials Science and Engineering at the Georgia Institute of Technology in Atlanta (USA) under the supervision of Prof. Juan Pablo Correa. Her research is focused on the design and synthesis of new organic hole-transporting materials and self-assembled molecules to analyse the connection between the structure and photovoltaic performance.

a power conversion efficiency (PCE) of 25.8% (*vs.* 3.8% in 2009), comparable to the current record certificated for traditional crystalline silicon solar cells (26–27%).[2] Among the advantages that have caught the attention and interest of many researchers are their high efficiency, low-cost manufacturing, versatility (shapes, colors, and flexibility) or their potential to combine with either c-Si, CIGS, organic or other existing solar cells in multijunction devices (tandem cells). In addition, their high performance in low light conditions and compatibility with other renewable energy sources have pushed the further industrialization of PSCs.[3–7]

Such as other photovoltaic devices, PSCs are made of a multilayer device structure in which the active and light-absorbing layer (perovskite layer) is sandwiched between two charge transporting layers (CTLs), *i.e.*, hole transporting layer (HTL) and electron transporting layer (ETL).[8–10] According to the direction of the current flow, perovskite devices can be divided into two well-known architectures: regular (n-i-p) and inverted (p-i-n) configurations (Fig. 1). Although slightly higher PCE are currently achieved with the regular nip-structures,[11] the pin-type PSCs exhibit several attractive advantages, such as low-temperature fabrication process, high device stability, negligible hysteresis, and excellent compatibility with flexible and tandem devices.[12]

To design stable and efficient PSCs, the selection of the electron and hole transport layers, as well as the perovskite material, results are crucial. The light-absorbing perovskite material is represented with the general formula ABX_3, and its composition, morphology, and crystallinity are well optimized to boost the performance of PSC devices toward higher efficiency and stability.[3,13] The ETL promotes the collection of photogenerated electrons from the perovskite layer to the corresponding electrode, consisting of metal oxides (TiO_2, ZnO, SnO) for regular PSCs and hydrophobic [6,6]-phenyl-C_{61}-butyric acid methyl ester (PCBM) or its derivatives for inverted PSCs.[14–16] On the other hand, the 2,2′,7,7′-tetrakis[*N*,*N*-di(4-methoxyphenyl)amino]-9,9′-spirobifluorene (Spiro-MeOTAD) has been the most employed hole transport material (HTM) for regular PSCs. In the case of inverted PSCs, different HTLs have evolved from copper (CuI, $CuCrO_2$), nickel (NiO_x), and polymers such as (poly(3,4-ethylene dioxythiophene)polystyrene sulfonate (PEDOT:PSS) and poly[bis(4-phenyl)(2,5,6-trimethylphenyl)amine](PTAA)), to diverse organic small molecules (SMs), including the emerging self-assembled monolayers (SAMs).[17–20]

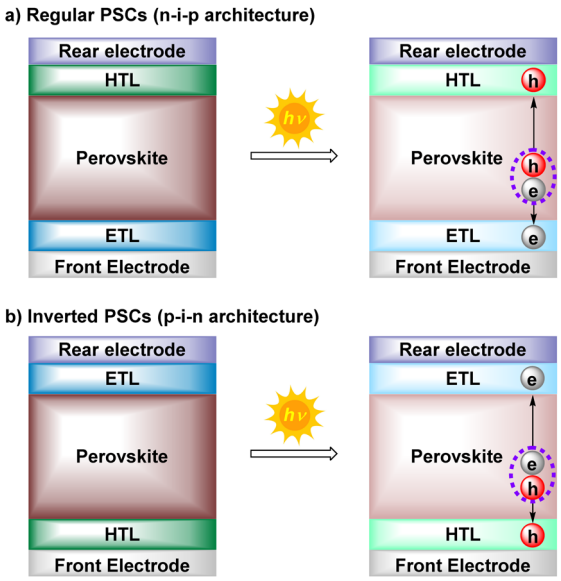

Fig. 1 Common architectures of PSCs (regular and inverted) and their working mechanism. h: holes, e: electrons.

Regardless of its composition, the role of these hole transport materials (HTMs) is (i) the extraction and transport of holes from the perovskite layer to the electrode;[21] (ii) establishing an energy barrier to block the flow of electrons, and thus, reducing recombination and current leakage;[22] and (iii) protecting the

Eugenia Martínez-Ferrero

Dr Eugenia Martinez-Ferrero holds a PhD in materials science from University of Valencia (Spain). She is currently scientific group coordinator in the group of Prof. Palomares at ICIQ, where she joined in 2021 after leading the optoelectronic device laboratory at Eurecat, a technological centre of Catalonia (Spain), for 10 years. Her background is on materials science and optoelectronic devices such as solar cells or light emitting devices. She is interested in establishing the relationship between the features of the materials and performance of the devices, in terms of efficiency and/or stability, a field where she has co-authored 76 publications.

Emilio Palomares

Dr Emilio Palomares is ICREA Professor and group leader at ICIQ who became director of the Institute in 2020. He has extensive experience in the design and synthesis of materials for energy and the construction of third generation solar cells of different nature such as organic, quantum dot, dye sensitised or perovskite based. He was awarded in 2009 with an ERC Starting Grant and, in 2023 with an ERC Advanced Grant. Prof. Palomares has co-authored more than 200 peer-reviewed scientific papers on molecules and materials for energy-related devices.

perovskite layer from moisture and oxygen, improving the device stability by reducing corrosion.[23] Although several works focused on the development of different HTMs are available in the literature,[24–28] it is worth mentioning that the design principles and the desired properties of the currently used HTMs differ substantially between regular (n-i-p) and inverted (p-i-n) architectures.

Among all the HTLs, during the last 5 years, special attention has been put to the development of self-assembled molecules as HTMs. These ordered arrays of organic molecules with a thickness of one or a few molecules have promoted the fabrication and study of efficient perovskite devices, the so-called SAM-based PSCs. Considering the accelerated growth, and the importance of organic chemistry in the design of these organic molecules, in this review we will cover the current challenges for the design and synthesis of SAMs for perovskite solar cells. The present review will be divided into three main topics: (i) the structural features that define a SAM, and how each part of the molecule has a counterpart and interacts with other layers; (ii) a quick overview of all commercial SAMs that have been used from the beginning, and how they have inspired the synthesis of new and complex SAMs to pursuit better efficiencies; and (iii) we will discuss all the synthetic protocols, mostly reported in the Supporting information of already published articles, to discuss their pros- and cons- and enhance the role of organic chemistry in this field, guiding the synthetic chemists to develop novel structures and benign procedures that promote the industrialization of PSCs.

Self-assembled molecules (SAMs)

Low molecular weight organic molecules (so-called "small molecules") can be used as HTMs under two different approaches: first, as a randomly deposited non-ordered array of planar and extended π-conjugated organic molecules deposited as a layer, or, as an ordered array of organic molecules with a very low thickness creating a layer that is well-known as a self-assembled molecule (SAM) (Fig. 2). The concept of SAMs was first described in the 1940s when a method to adsorb surfactants on different metal surfaces was reported. Then, in 2014, it was first applied in the fabrication of PSCs,[29] when benzoic acid and a fullerene derivative were used in inverted (p-i-n) configurations,[30] inspired by the results obtained in polymer solar cells.[31–33]

The formation of SAMs is a thermodynamically favorable process depending on two main aspects: (i) the adsorption of each molecule to a specific surface, and (ii) the intermolecular interactions that form the unidirectional monolayer.[34,35] Nevertheless, the most attractive feature of SAMs is that each molecule that conforms to the monolayer can have a specific functional group, resulting in a highly functionalized, packed, and ordered unidirectional monolayer with different properties deposited on a desired surface. The combination and control of these three remarkable aspects of SAMs can be easily tuned varying the chemical structure of the molecules that form the SAMs. Therefore, it is in this field that organic chemistry plays an important role in the design and synthesis of the molecules that will be an important part of perovskite devices.

Thus, the structural requirements needed for a molecule to be able to form a SAM are an anchoring group, that allows the chemical adsorption onto the surface, a linker or spacer moiety, to assist and promote the self-assembly process, and a functional group, to modify the nature of the monolayer and trigger all the possible interactions with the overlayer in the PSCs device (Fig. 3).

The anchoring group is involved in the bonding interactions of each molecule to the surface through chemical reactions such as hydrolysis and condensation.[36] For PSCs the most used and common anchoring groups are Brønsted–Lowry acids such as the carboxylic acids (–COOH) and phosphonic acids (–$PO(OH)_2$) that can allow mono-, bi-, and tridentate binding modes, depending on the surface type.[37]

The spacer group, besides being the bridge between the anchoring and the functional groups, is in charge of developing a well-organized molecular packing during the self-assembly process *via* van der Waals forces. Thus, inactive aliphatic and conjugated benzene rings, of different sizes and lengths, are often used as spacer groups.[38]

Finally, the functional group will define the nature of the new monolayer. Inspired by other HTMs, these groups are responsible for all the physical and chemical interactions at the interface, which in most cases is in contact with the perovskite layer, so these functional groups create a template for the deposition of the next layer, influencing in its structure and morphology. Different nitrogen, sulfur, and oxygen heterocycles and some organic cations that possess strong interaction with the perovskite frameworks are the most common groups used in PSCs.[39]

The deposition techniques (vapor deposition, dip-coating, and spin-coating methods), characterization, and role in the

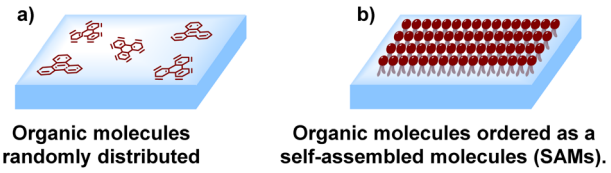

Fig. 2 Organic small molecules as HTMs in different organizations: (a) random or (b) as SAMs.

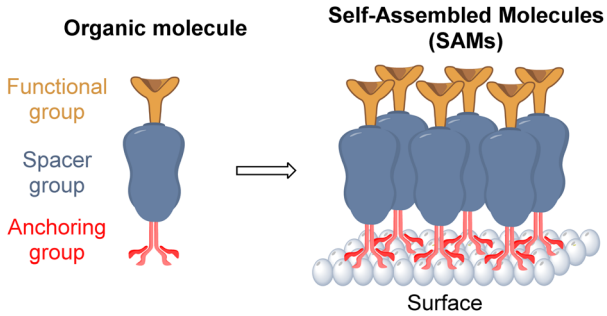

Fig. 3 Structural components of the SAM and self-assembly process to form the monolayer.

electronic function and performance of PSCs of SAMs are well documented in the literature.[38–41] The presence of an anchoring group and a functional group, with different electron densities and separated by the spacer group, in the chemical structure of the molecules that form SAMs, results in a monolayer with a specific dipole that could decrease or increase the work function of the metal surface containing the SAM.[42] The spacer group governs the charge transport at the interface, determining the electronic conductivity and optical properties of the PSCs.[43] While the functional groups, beyond interacting with the overlayer, contribute to the energy level alignment (HOMO–LUMO) between the SAM and the perovskite, and add additional surface dipoles that contribute to the changes in the work function.[44] Other important effects of SAMs in the performance of PSCs are: improving the crystal quality of the perovskite layer reducing the degree of defects, protecting the perovskite layer isolating it from the metal contact, and reducing the undesired charge recombination. Noteworthy, the low cost of the material and low material consumption during the fabrication of large-area perovskite devices, makes the design and synthesis of organic molecules, for the preparation of SAMs, an interesting and promising field to contribute to the study and industrialization of PSCs.

Commercial self-assembled molecules (SAMs)

Before organic chemists became interested in the design and preparation of molecules to form SAMs, several research groups recognized the potential of SAMs for the development of efficient photovoltaic devices. By that time, those studies were based on different simple and easily commercially available compounds as a platform to make progress in the formation (deposition techniques), characterization (IR, X-ray, SEM, contact angle, *etc.*), role (conductivity, passivation, template, work function, *etc*) of SAMs for the fabrication of perovskite solar cells.

These pioneer works not only established the structural parameters that a molecule must have to be considered as a promising building block for SAMs, but also, inspired the organic chemists to actively participate in the molecular design of novel chemical entities, proposing and exploring different

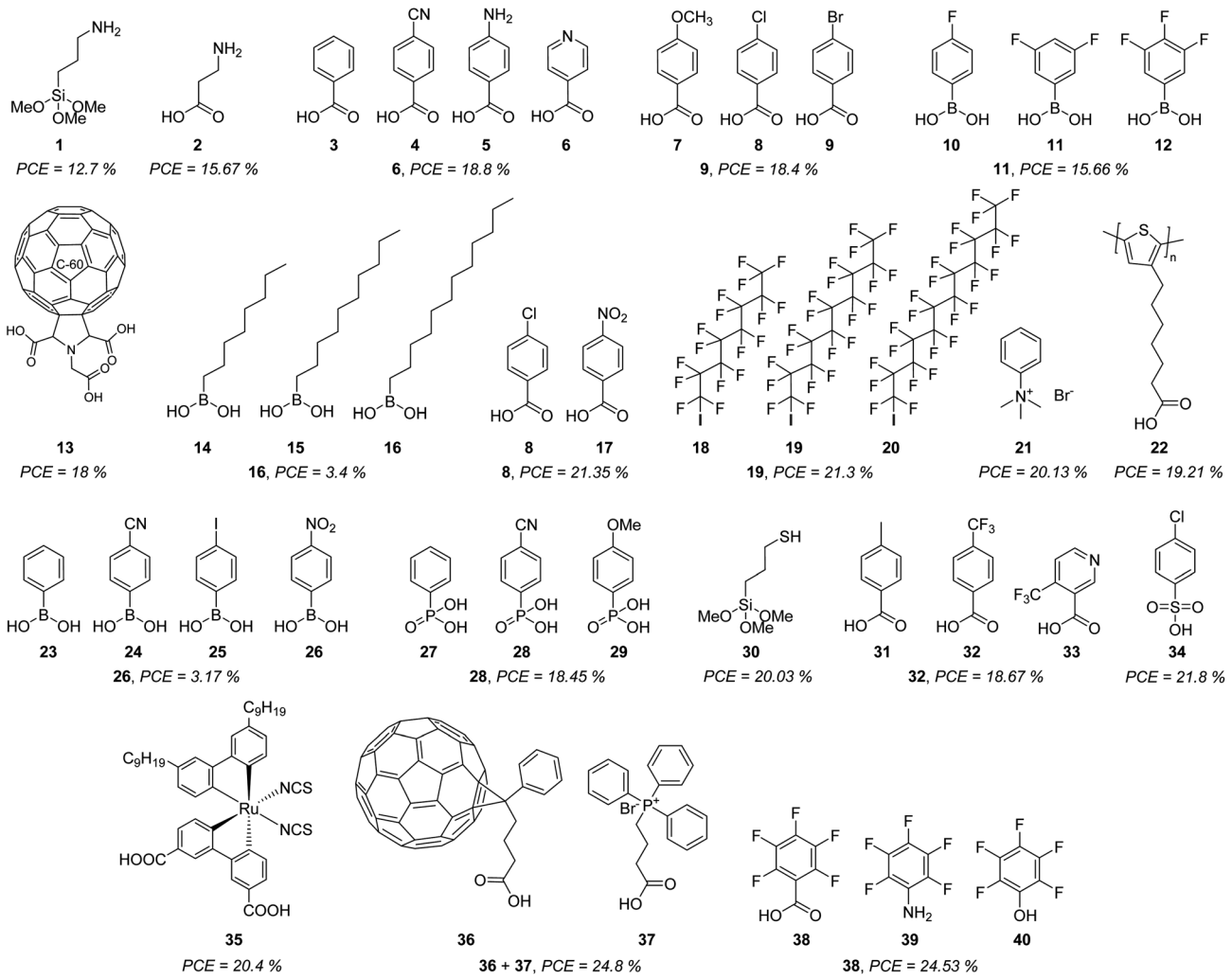

Fig. 4 Commercial molecules are used for the formation of SAMs in PSCs, indicating the highest PCE obtained in each case.

anchoring, spacer and functional groups, creating interesting combinations between them, and reaching outstanding PCEs and stable PSCs.

Although nowadays one of the main topics in the field is the design and synthesis of small molecules to form SAMs for PSC devices, some interesting works continue exploring commercial compounds with remarkable results. The library of available molecules used for SAMs is quite vast, and it has been well described in the literature,[38,39] however in this section we selected some of the relevant molecules, that in our opinion, have inspired most of the synthesis of novel derivatives, according to their chemical structure (Fig. 4).

The first report based on the use of a commercial SAM in PSCs backs to 2015, where aminopropyltrimethoxysilane **1** was used to incorporate a SAM between the TiO_2 and $CH_3NH_3PbI_3$ perovskite, obtaining a PCE of 12.7% with a SAM composed of silane groups as an anchoring group, a propyl chain as linker and a primary amine as a functional group.[45] At the same time, ZnO-coated glass/ITO substrates were modified with a SAM formed by 3-aminopropanioc acid **2**, and the PCE was improved by 15.6% by using carboxylic acids as anchoring groups and reducing the length of the linker group.[46] This study inspired the use of some benzoic acid derivatives **3–9** where the most efficient result was 4-pyridine carboxylic acid **6** with a PCE = 18.8%, demonstrating that ternary amines or aromatic *N*-heterocycles were better functional groups than primary amines,[47] while 4-bromobenzoic acid **9** demonstrated to have a positive effect passivating the surface, reducing the recombination and minimizing the energy offset between NiO_x nanoparticles and the perovskite in both, regular and inverted devices.[48]

The acidity of carboxylic acid function as an anchoring group results in a problem for the stability of the PSCs, due to the corrosion that induces. To reduce this negative impact, boronic acids were tested as an anchoring group where the best results were obtained with the 3,5-difluoro derivative **11** (PCE = 15.66%).[49]

The localization of positive ions caused by hydroxyl groups present at the metal surface (SnO_2, TiO_2, *etc.*) increases hysteresis and degradation of the device. Thus, to prevent this event, the respective C_{60} pyrrolidine **13**, with 3-carboxylic acid functions, was used as a SAM for the fabrication of a PSCs device that resulted stable after 1000 h of continuous illumination without any significative decrease in the PCE.[50]

Aliphatic boronic acids **14–16** of different chain lengths, and without any functional group, demonstrated that the charge transport properties were enhanced from C_8 to C_{12}, although very low PCE was achieved (3.4%).[51]

Exploring other benzoic acid derivatives, but using TiO_2 as a substrate and Cs_8FAMA as a perovskite layer, afforded efficient PSCs devices when 4-chlorobenzoic acid **8** was employed as a SAM (PCE = 21.35%), while derivatives with electron-withdrawing groups such as nitro group (-NO_2) **17** resulted in very inefficient devices (PCE = 1.01%) in both, regular and inverted configurations.[52]

Usually, the SAM layer is deposited below the perovskite layer. However, a self-assembled monolayer could also be formed on top of the perovskite layer to encapsulate and protect the active material. This was achieved with perfluorinated aliphatic carbon chains of different lengths **18–20** and terminated with an iodine atom as the anchoring group, finding that a C_{12}-carbon chain exhibited a PCE of 21.3%.[53] Another example of the formation of SAMs on top of the perovskite layer was reported with the phenyltrimethylammonium bromide **21**, which successfully passivated the PbI_3^- defects and enhanced the photovoltaic properties and stability of the device with a PCE of 20.13%, exhibiting a PCE = 17.31% after 60 days.[54]

A monolayer of self-assembled molecules can be formed as well by polymers as reported for poly[3-(6-carboxyhexyl) thiophene-2,5-diyl] **22** that formed an ordered and homogeneous monolayer promoting the growth of high-quality perovskite film in a device that exhibited a PCE of 19.21%, being stable for 5000 h.[55]

Despite their low PCE, boronic acids continue to captivate attention as a precursor of SAMs. Although the nitro group demonstrated to be less efficient when carboxylic acids were used as an anchoring group **17**, when boronic acids were employed instead, the changes in the dipole and the work function induced by (4-nitrophenyl)boronic acid **26** resulted in a slight improvement of the PCE for this kind of PSCs (PCE = 3.17%).[56]

Phosphonic acids are one of the best anchoring groups that can be used in the formation of SAMs for PSCs, since they strongly attach, through one-, two-, or three binding sites, to different metal surfaces. This was demonstrated by a series of *p*-substituted phenylphosphonic acids **27–29** on NiO_x-ITO substrates, where the best results were obtained from the cyano derivative **28** with a PCE of 18.45%.[57]

Sulphur is one of the atoms that have shown great affinity for lead-based perovskites, because of the S···Pb interactions, many crystallization defects are covered by sulphur. For example, 3-mercaptopropyltrimethoxysilane (MPTMS) **30** formed a SAM in regular PSCs devices on SnO_2 reaching a PCE of 20.03%, enhancing the extraction efficiency of photogenerated electrons and restraining recombination.[58]

Due to its small size and strong electron-withdrawing property, fluorine influences the perovskite crystallization kinetics and regulates the properties of the interface more than other functional groups. This was observed in the series of compounds **31–33** where 4-(trifluoromethyl)benzoic acid **32** improved the PCE to 18.67% and a high open-circuit voltage (V_{OC}) of 1.160 V was achieved with a significant decrease of the defects and non-radiative recombination.[59]

Although less common, sulphonic acids can also be promising anchoring groups, as in the case of *p*-chlorobenzenesulfonic acid **34** which mitigates two of the most adverse problems in NiO_x-based inverted perovskites. On one side, the chlorine functional group of **34** promotes perovskite growth, while the sulfonic acid group passivates the surface defects detected in NiO_x, reaching a PCE of 21.8%.[60]

One of the benchmark sensitizers widely employed in dye-sensitized solar cells (DSSCs) has been recently used to promote the formation of SAM in PSCs. The Z907 dye **35** is an amphiphilic ruthenium dye that is chemically and

spontaneously absorbed on the TiO_2 forming a monomolecular layer that allows the fabrication of a perovskite device with low energy loss and higher interface coupling with the perovskite. In addition, the obtained SAM built a back surface field through a p-type doping effect that promoted the hole extraction and suppressed the carrier recombination, resulting in a PCE of 20.4%, a high value for a transition metal-SAM.[61]

But SAMs cannot only be formed by one single molecule, in 2023. It was demonstrated the synergic effect of combining [6,6]-phenyl-C_{61}-butyric acid **36** and 3-carboxypropyl-triphenyl phosphonium bromide **37** to form a monolayer where the strong fullerene **36** interactions promoted the ordered array of **37**. The resulting monolayer simultaneously influences defect passivation and improves carrier transportation in a PSC device to reach a PCE of 20.4%.[62]

Finally, and more recently, a series of simple polar molecules **38–40**, with permanent dipole moments and different anchoring groups, were used to modify the perovskite surface through a SAM approach. Once again, the role of the fluorine atom becomes relevant, especially the pentafluoride benzene moiety, because of its hydrophobicity that protects the perovskite layer from water. On the other hand, the dipoles at the interface produced an offset in the vacuum level, leading to PSCs with a PCE of 24.53% for molecule **38**, which possessed the carboxylic acid function as an anchoring group (Fig. 4).[63]

The chemical structures depicted in Fig. 4 are just correlated with the power conversion efficiency (PCE) achieved by each molecule in different PSC devices. Nonetheless, we want to state that other important parameters are needed to take into account for evaluating the performance of those devices, such as the work function (WF), open circuit voltage (V_{OC}), current density (J_{SC}), and fill factor (FF), so we encourage the readers to examine these excellent works and also get inspired to design new molecules that can be used as SAM.

The success of small organic molecules and SAMs is not exclusively for PSCs, indeed some commercial molecules such as fluorobenzoic phosphonic acids have been deposited on ITO surfaces for the fabrication of organic light-emitting diodes (OLEDs).[64] While techniques such as atomic layer deposition (ALD) have been employed and explored for the formation of high-quality self-assembled molecules (SAMs) using octadecylphosphonic acid in other photovoltaic applications.[65]

In the following sections, we will discuss in detail the protocols developed for the preparation of the most promising synthetic molecules, according to their main structural features, reported so far for the formation of SAMs in perovskite solar cells, including some interesting examples that are already patented and commercialized.

C_{60}-SAMs

To the best of our knowledge, 2014 was reported as the first SAM for PSCs inspired by previous works on polymer solar cells, where fullerene derivatives proved to be efficient.[66] Thus, the C_{60}-substituted benzoic acid **44** (Scheme 1) was used for regular PSC devices reaching a 17.3% PCE with significantly reduced hysteresis. Compound **44** was synthesized through a 1,3-dipolar

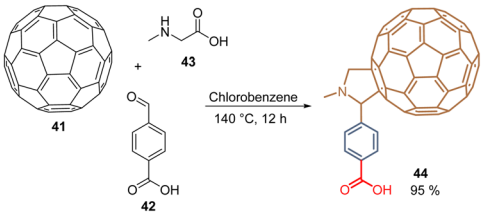

Scheme 1 Synthesis of C_{60}-SAM **44** through Prato reaction. (Red) Anchoring group; (Blue) spacer group; (Brown) functional group.

cycloaddition reaction, known as a Prato reaction, between C_{60} **41**, 4-carboxybenzaldehyde **42**, and *N*-methylglycine **43** using chlorobenzene as a solvent under reflux for 12 h. This reaction yielded the desired fullerene **44** functionalized with the carboxylic acid function as an anchoring group in 95% (Scheme 1).[67] Derivative **44** is now commercialized under the name C_{60}-SAM (CAS No. 631918-72-4) and was recently used for the fabrication of regular (n-i-p) perovskite/silicon tandem solar cells with a PCE of 27.1%.[68]

Using a molecular hybridization strategy, where two molecular entities are bonded through a specific linker. Derivative **49** was prepared to employ a click chemistry strategy, where the commercially available C_{60}-carboxylic acid **45** was subjected to an esterification process with the corresponding 10-undecyn-1-ol **46** to give the functionalized C_{60} intermediate **47** in 75% yield. Then, it reacted with the respective dihydroxy azide **48** under the traditional reaction conditions for the azide–alkyne Huisgen cycloaddition, furnishing the fullerene diol **49** in 56% yield (Scheme 2). SAMs were formed on tin oxide (SnO_2) surfaces, using the diol fragments as an anchoring group, for the fabrication of planar heterojunction perovskite solar cells with PCE = 21.3%, that resulted in stable and displayed a negligible hysteresis.[69] Employing the Prato reaction for the functionalization of fullerenes, compound **52** was designed and prepared based on C_{60}-SAM **44**, selecting the cyano group as an anchoring group to enhance the solubility of these derivatives and adding a thiophene ring into the pyrrolidine core to promote the interaction of the perovskite material and the sulfur atom and π–π interactions. Thus, **52** was isolated in 44% yield from C_{60} **41**, *N*-(2-cyanoethyl)glycine **50**, and 2-thiophenecarboxaldehyde **51** after 22 h at 135 °C (Scheme 3). Derivative **52** was used as an ETM in PSCs to achieve a PCE of 20.58%, which is one of the highest values reached for fulleropyrrolidine analogs reported to date in PSCs.[70]

Fullerenes are widely used in the construction and study of efficient PSCs, improving stability, lowering the hysteresis, and increasing the PCE.[71] Although phenyl-C_{61}-butyric acid methyl ester (PCBM) is one of the most common fullerene-based materials used in PSCs, it is mainly employed nowadays as an ETM instead of a SAM. In this sense, the Prato reaction stands out as one of the best approaches for the synthesis of fullerene-based molecules that can be used as SAM in PSCs, however, two main challenges need to be addressed: (i) explore the structural diversity of the starting materials, and (ii) study the reaction conditions, to decrease the reaction temperatures and use

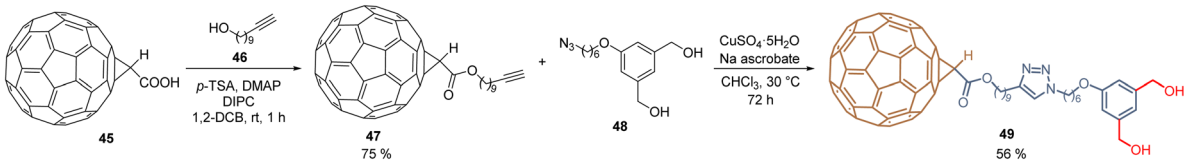

Scheme 2 Click chemistry approach for the functionalization of fullerene core and synthesis of fullerene diol **49**.

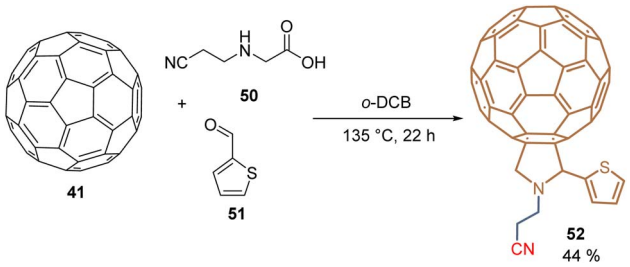

Scheme 3 Prato reaction for the synthesis of fulleropyrrolidine **52** substituted with the thiophene moiety.

alternative solvents to replace traditional halogenated aromatic hydrocarbons.

Carbazole-SAMs

Carbazole is a tricyclic ring system based on a pyrrole ring fused with two benzene rings, and it is the presence of the electron-rich pyrrole ring that one responsible for the hole-transporting properties of this inexpensive starting material. Due to its substitution pattern, carbazoles can be easily functionalized at the nitrogen and the "benzene" rings, furnishing a huge library of small molecules and polymers with applications in photovoltaics.[72] Carbazole exhibits good charge transporting ability, chemical stability, and electronic and optical properties that can be tuned by well-known organic chemistry processes, which has attracted researchers to design molecules as SAMs for PSCs.[73,74]

The first example of a carbazole-based HTM modified with a phosphonic acid as an anchoring group used as a SAM was prepared in 2018 from carbazole **53**.[75] The synthesis of **58** involved 5 steps starting with the bromination of carbazole **53** to furnish 3,6-dibromocarbazole **54** (>99%), that was then alkylated with 1,2-dibromoethane to give the intermediate **55** with yield over 90%. The subsequent transformation of the aliphatic bromide into the corresponding phosphonic acid ethyl ester **56** was performed through the Arbuzov reaction with excellent yield. In the next step, the dimethoxydiphenylamine fragments were introduced *via* palladium-catalyzed Buchwald–Hartwig amination reaction to give the derivative **57** in moderate yield. Finally, bromotrimethylsilane (TMSBr) was used to cleavage the ester functions and obtain the desired carbazole derivative **58** in 86% (Scheme 4). Compound **58**, known as a V1036, was obtained in 46% global yield and formed a layer of SAMs onto indium tin oxide (ITO) surfaces through the phosphonic acid group that acted as an anchoring group, giving a PCE of 17.8% in p-i-n PSCs devices.

Certainly, the later application in 2019 of [2-(9*H*-carbazol-9-yl)ethyl]phosphonic acid (2PACz) constituted a breakthrough in the development of PSCs, since the prepared devices outperformed the traditional polymer PTAA. In comparison to V1036 **58**, the structure of 2PACz **61** is quite simple, and this compound and its derivatives have allowed us to prepare devices with excellent efficiencies and stability. The synthesis of 2PACz **61** and its derivatives **65–71** follows the same approach as for V1036 **58**, involving the *N*-alkylation with 1,2-dibromoethane, then the Arbuzov reaction and finally the cleavage of the ethyl groups to obtain the anchoring group (Scheme 5). In the case of 2PACz **61**,[76] it was prepared from carbazole **53** in a 3-step lineal synthesis in 40% global yield, and although the first PCE reported was 20.9% for a SAM formed in Pb–PSCs, recently, 2PACz **61** was absorbed with methyl phosphonic acid to fabricate a Sn–Pb PSC with a PCE of 23.3% (Scheme 5).[77]

For the insertion of the methoxy groups, intermediate **54** was transformed into the corresponding 3,6-dimethoxy-9*H*-carbazole **62** through a Cu-catalyzed methoxylation reaction in 63% yield,[78] then the same approach was performed to obtain the MeO-2PACz **65** after 5 steps and in 28% global yield (Scheme 5).[76] The presence of methoxy donor groups in MeO-2PACz **65** resulted in PSCs with a slightly lower PCE of 20.2% in the first study. However, currently, the synergy between 2PACz **61** and

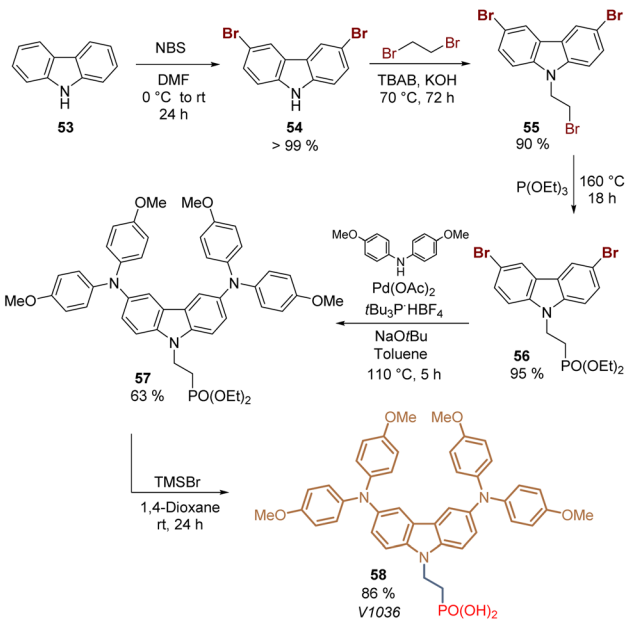

Scheme 4 Synthesis of V1036 **58**, the first carbazole-based SAM in PSCs.

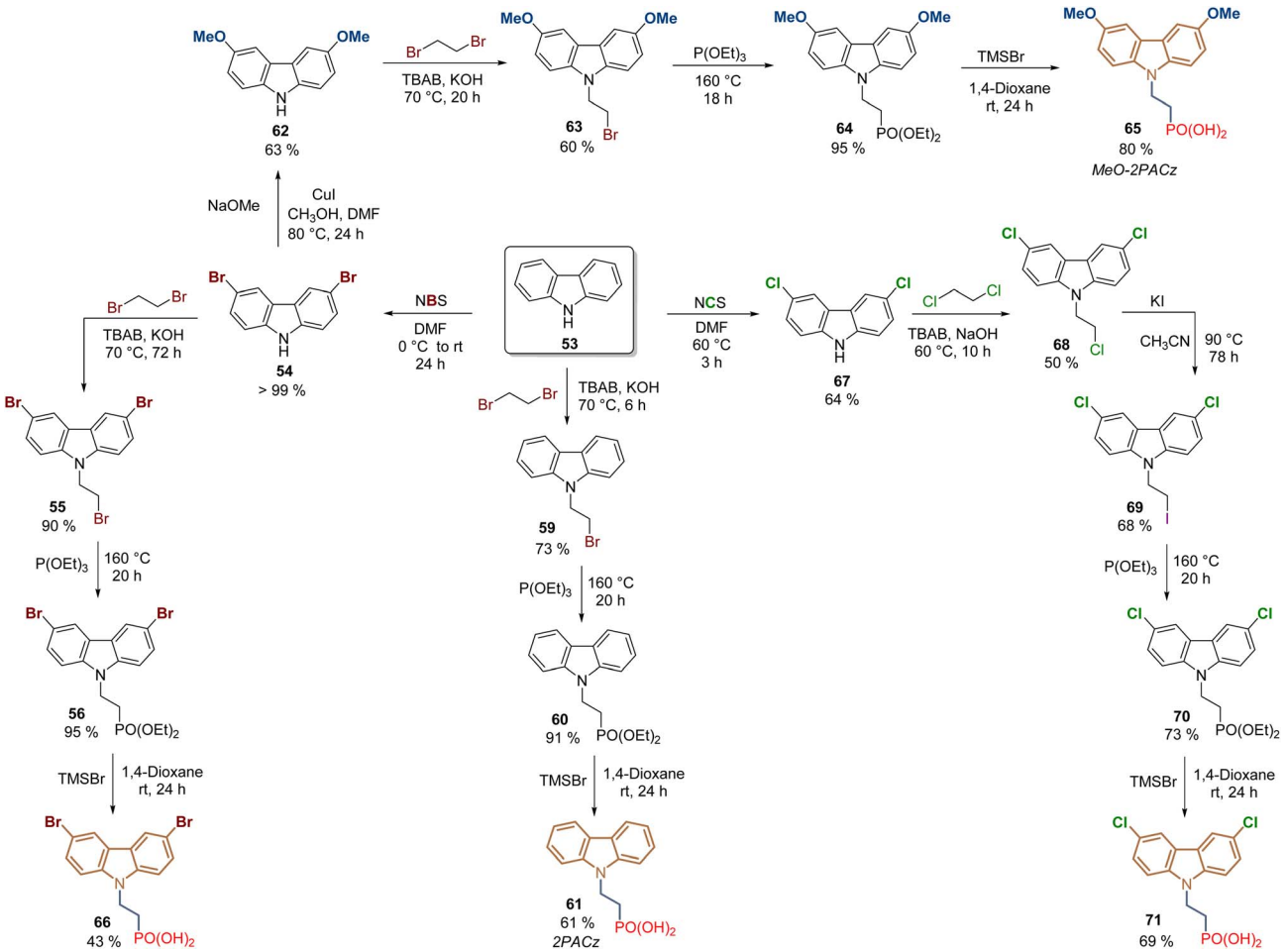

Scheme 5 Synthesis of 2PACz **61** and its derivatives under the reactions sequence: halogenation/*N*-alkylation/Arbuzov reaction.

MeO-2PACz **65** is successfully applied, so when they are combined, mixed layers of SAMs are formed where the uncovered areas of one molecule are filled with the other, allowing the fabrication of flexible PSCs (PCE = 24.7%)[79] and perovskite-silicon tandem solar cells (PCE = 28.3%).[80]

To modify the electronic nature of 2PACz **61**, by introducing electron-withdrawing groups such as bromine and chlorine, compounds **66** and **71** were prepared under the same approach. The dibromo derivative **66** was obtained in 36% global yield after 4 steps from carbazole **53** and a PCE = 18.4% was reported for the PSCs devices where the SAM layer was formed on ITO surfaces.[81] Although **71** was prepared to form a SAM for perovskite light-emitting diodes (PeLEDs), the synthesis of this dichloride derivative has been also reported under the same protocol but using *N*-chlorosuccinimide (NCS), however, the use of 1,2-dichoroethane for the *N*-alkylation required an additional step to exchange the halogen and increase the reactivity of **69** towards the Arbuzov reaction.[82]

2PACz **61** (CAS No. 20999-38-6) and MeO-2PACz **65** (CAS No. 2377770-18-6) are now commercially available references. However, it is worth mentioning that, as an alternative approach, in our group the synthesis of 2PACz analogs is carried out with the commercial diethyl 2-bromoethyl phosphonate as a starting material, reducing the synthetic steps and reactions carried out at high temperatures for prolonged times.

New derivatives have been explored to study the effect of the length of the spacer group applying the synthetic protocol of 2PACz **61**, as a starting point. Thus, a series of derivatives with 2C, 4C- and 6C-aliphatic chains between the anchoring and the function group, were designed, synthesized, and applied in devices, revealing an optimum value of the fill factor for 2C and 4C derivatives. On the other hand, current–voltage hysteresis was observed in the devices prepared with SAMs of the 6-carbon chain independently from the substituent at the carbazole core.[83] In this study, the methylation of 3,6-dibromocarbazole **54** was performed under Ni-catalysis in moderate yield and after the halogenation/N-alkylation/Arbuzov reactions sequence, the series of derivatives **75a–e** were obtained in good to excellent global yields (Scheme 6). Compound **75b** proved to be the most promising derivative to form a layer of SAM on ITO surfaces for the fabrication of monolithic perovskite/silicon tandem cells with a PCE of 29.15%.

Another important study based on the structure of MeO-2PACz **65** was focused on the insertion of the methoxy groups at different positions in the carbazole core. Thus, introducing the methoxy groups at positions 2 and 7, instead of 3 and 6,

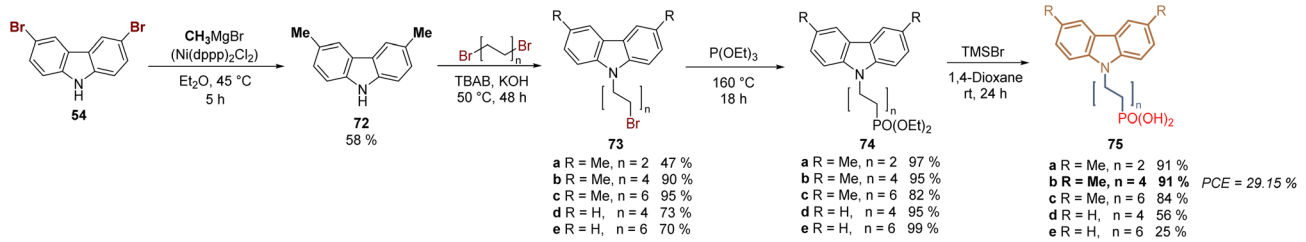

Scheme 6 Synthesis of 2PACz-based molecules **75a–e** with different spacer group lengths, $n = 2$, 4 and 6.

allowed the preparation of compound **80** from the commercial carbazole **76** using diethyl 2-bromoethyl phosphonate **78** for the *N*-alkylation, furnishing the desired product in 36% global yield over 4 steps (Scheme 6). The authors found that the change in the position of the methoxy groups resulted in the reduction of the electron-donating strength in comparison to MeO-2PACz **65**. This effect downshifted the highest occupied molecular orbital (HOMO) energy creating a favorable dipole moment. Thus, derivative **80** was combined with 6-(iodo-λ^5-azanyl) hexanoic acid (IAHA) to form a SAM in inverted PSCs reaching a PCE = 23.59% (Scheme 7).[84]

In 2021, our group reported for the first time the use of aromatic rings in the spacer group in carbazole-based SAMs for PSCs. These molecules were designed inspired by our previously reported HTMs based on the triphenylamine moiety,[85] and included the 1,3-dimethoxybenzene substituent at the carbazole core to align the energy levels of the molecules with the perovskite material. The synthesis started with the bromination of carbazole **53** followed by the double Suzuki coupling to give the disubstituted intermediate **82** in 90% yield. This was subsequently subjected to the Buchwald–Hartwig amination with bromo benzoic acid esters derivatives that, upon hydrolysis, furnished the derivatives **83** (89%) and **84** (48%). Each molecule had one and two aromatic rings as spacer groups, respectively, with the carboxylic acid function as an anchoring group (Scheme 8).[86] Both molecules formed good quality SAM layers on ITO giving outstanding efficiencies and excellent lifetimes. The derivative **83**, also known as EADR03, gave PCE of 21.2% and is currently commercialized while the derivative **84**, EADR04, has demonstrated promising results in the increase of the efficiency and lifetime in PeLEDs.[87]

Conjugated and aromatic spacer groups exhibit effective hole-transporting capabilities in comparison with the aliphatic linkers, along with higher stability due to the stabilization of the electron-rich carbazole core through electron/charge delocalization. This was also demonstrated with a series of molecules containing the same functional group that MeO-2PACz **65**, but with one and two aromatic rings as a spacer group, in addition to the cyanoacetic acid moiety as an anchoring group. Compounds **88** and **91** were prepared from 3,6-dimethoxy-9*H*-carbazole **62** through a Ullmann-type reaction to give the *N*-phenyl carbazole intermediates **87** and **88** good to excellent yields (Scheme 9). Carboxaldehyde derivative **87** was subjected to a traditional Knoevenagel condensation with cyanoacetic acid to furnish the final product **89** in 48% global yield, while the bromine analog **88** was transformed into the corresponding carboxaldehyde intermediate *via* Suzuki coupling in 74% yield to finally introduce the anchoring group, obtaining the compound **91** in 35% global yield. Both molecules formed SAM layers on ITO giving similar results in terms of efficiency (PCE ≈ 20%), slightly lower in comparison to analogues **83** and **84**. However, it is important to highlight that the strong electron-withdrawing properties of this anchoring group resulted in

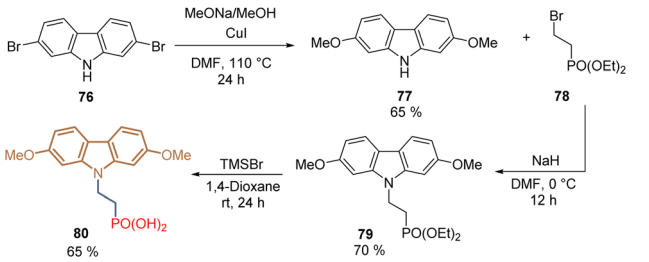

Scheme 7 Synthesis of MeO-2PACz analog **80** substituted in positions 2 and 7.

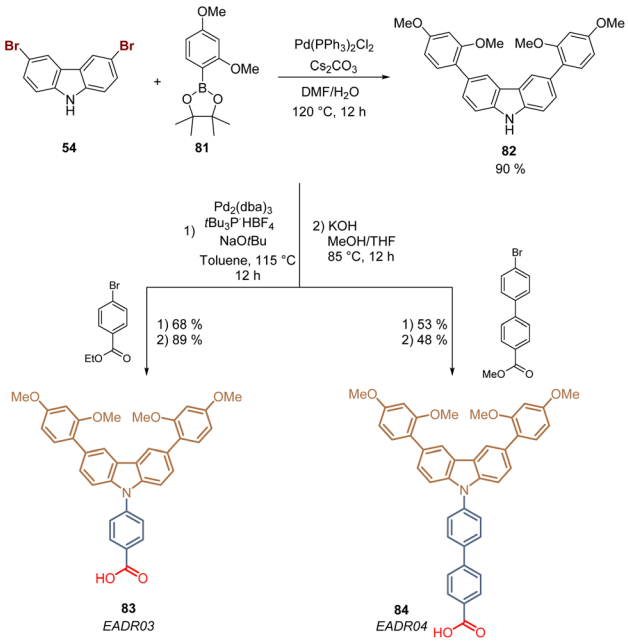

Scheme 8 Introduction of aromatic rings in the spacer group of molecules **83** and **84**.

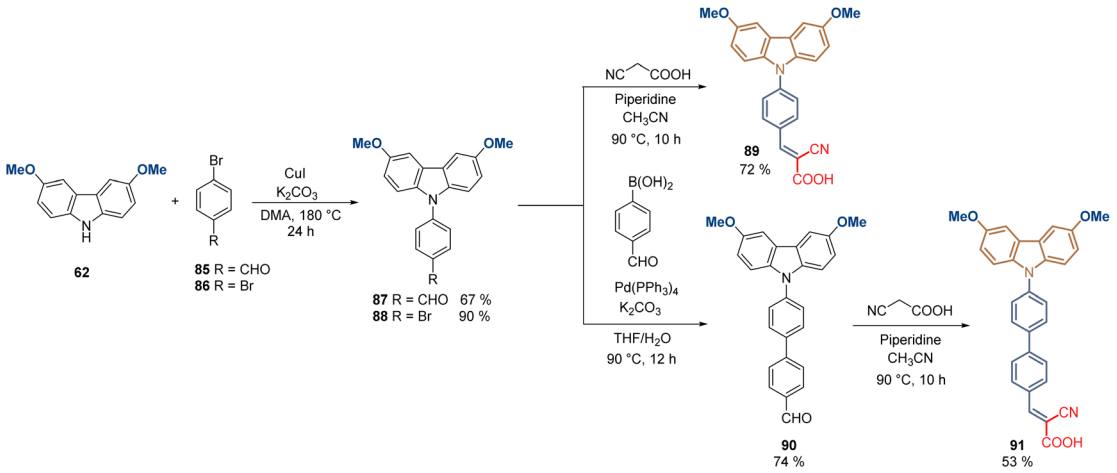

Scheme 9 Synthesis of molecules **89** and **91** with conjugated spacer groups and cyanoacetic moiety as anchoring group.

beneficial charge delocalization, and the passivation of the perovskite material due to the presence of the –CN.[88]

One of the latest structural modifications performed on the 2PACz **61** structure has been the asymmetric and helical π-expansion of the carbazole core and the use of a 4C aliphatic chain as a spacer group to obtain derivatives with higher dipole moment and strengthen the π–π interactions. Under this approach, commercially available 7*H*-benzo[*c*]carbazole **92** and 7*H*-dibenzo[*c*,*g*]carbazole **93** has been employed as starting materials to perform the reaction sequence: *N*-alkylation/Arbuzov reaction/deprotection, giving the corresponding (4-(7*H*-benzo[*c*]carbazol-7-yl)butyl)phosphonic acid **98** (asymmetric π-expansion) and (4-(7*H*-dibenzo[*c*,*g*]carbazol-7-yl)butyl) phosphonic acid **99** (helical π-expansion) in 66% and 63% global yield, respectively (Scheme 10). Both compounds exhibited excellent photo and thermal stability under sunlight and at temperatures above 366 °C. A PCE of 24.1%, with improved device stability was achieved by compound **99** in an inverted PSC. The higher dipole moment of **99** (2.4 D-calculated), down-shifted the WF to −5.15 eV and induced a more efficient hole extraction to achieve a FF of 83.39% and a V_{OC} of 1.17 V.[89]

The derivative **99** stands out as one of the most promising SAMs for PSCs, indeed, this compound has been also recently used to form a SAM layer in perovskite tandem solar cells with a PCE = 27.0%, FF = 82.6 and V_{OC} 2.12 V.[90]

In conclusion, carbazoles have shown their potential to act as excellent cores for the synthesis of HTMs with application in perovskite solar cells, increasing the PCE from 17.8 to 24.1%. Despite its low cost, high carrier mobility, chemical stability, and easy functionalization, the commercialization of the carbazole derivatives will come with the improvement of cost-effective synthetic methods. On the other hand, the increase in the PCEs will require the exploration of other functional groups along with the study of cost-effective synthetic protocols.

TPA-SAMs

The triphenylamine (TPA) group is a strong electron donor moiety commonly employed in molecules used as an HTM in several optoelectronic applications such as organic light-emitting diodes (OLEDs), Dye-Sensitized Solar Cells (DSSCs), and organic field-effect transistors (OFETs). This fragment has a butterfly-like shape with a sp^2 central nitrogen that generates a non-planar structure, in comparison with the rigid carbazole core, controlling the packing of the molecules, which is very useful during the formation of layers of SAMs.[91]

The TPA fragments show good thermal and morphological stabilities, ionization potentials, as well as excellent charge transport properties.[92] The nitrogen atom in the TPA core can be easily oxidized and stabilized by hyperconjugation electronic effects, resulting in high hole mobilities. For these reasons, the TPA fragment is the main core in two of the most important HTMs used in PSCs nowadays: the 2,2′,7,7′-tetrakis[*N*,*N*-di(4-methoxyphenyl)amino]-9–9′-spirobifluorene (spiro-MeOTAD)[93] and the poly[bis(4-phenyl)(2,4,6-trimethylphenyl)amine] (PTAA).[94]

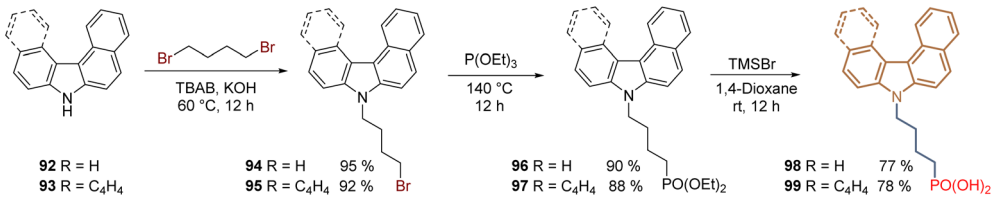

Scheme 10 Synthesis of π-expanded carbazoles **98** and **99** as an approach for the formation of stable and efficient SAMs.

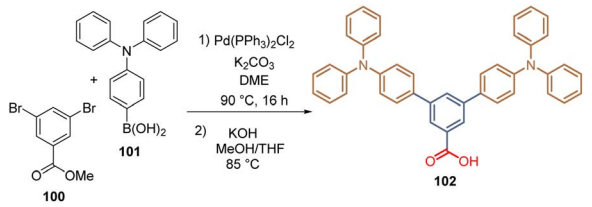

Scheme 11 Synthesis of the first molecule based on the TPA fragment for SAM in PSCs.

Inspired by our previous studies in DSSCs, our group reported for the first time the introduction of the TPA in two derivatives for the formation of SAMs for PSCs. The first molecule included two TPA fragments attached to a benzene ring, a spacer group, and a carboxylic acid function as an anchoring group.[95] The synthesis of this derivative involved the double Suzuki cross-coupling between methyl 3,5-dibromobenzoic acid **100** and 4-(diphenylamino)phenyl boronic acid **101** to give an intermediate that was then hydrolysed to obtain the desired compound **102** (Scheme 11).

The second molecule, **109**, prepared in our group was a structural analog of **84**, substituting the carbazole core with a TPA moiety, which is attached to the spacer group (two aromatic rings) and possesses two electron-donating fragments substituted with dimethoxy groups. The synthesis of **109** starts with the double Suzuki coupling between 4-bromo-*N*-(4-bromophenyl)-*N*-phenyl aniline **103** and 2-(2,4-dimethoxyphenyl)-4,4,5,5-tetramethyl-1,3,2-dioxaborolane **104**. The obtained intermediate **105** (92%) is then brominated with NBS in good yield (88%) resulting in the functionalized TPA fragment **106**, which upon a Suzuki reaction with [4-(methoxycarbonyl)phenyl] boronic acid **107**, gives the key intermediate **108** in 74% yield. Finally, the hydrolysis generates the corresponding anchoring group, and the desired compound **109** is obtained after 4 steps in 50% global yield (Scheme 12).[96] Molecules **102** and **109** formed layers of SAMs on ITO and were used in the fabrication of p-i-n PSCs. Due to the electron-donating groups introduced in the TPA backbone, a PCE = 17.3% was achieved because of the reduction of the oxidation potential of **109** in comparison to **102**. Although the PSCs devices fabricated with **84** and **109** have a different architecture, closing the TPA fragment and generating the pyrrole ring to form the carbazole derivative **109**, enhances the PCE to 20%.

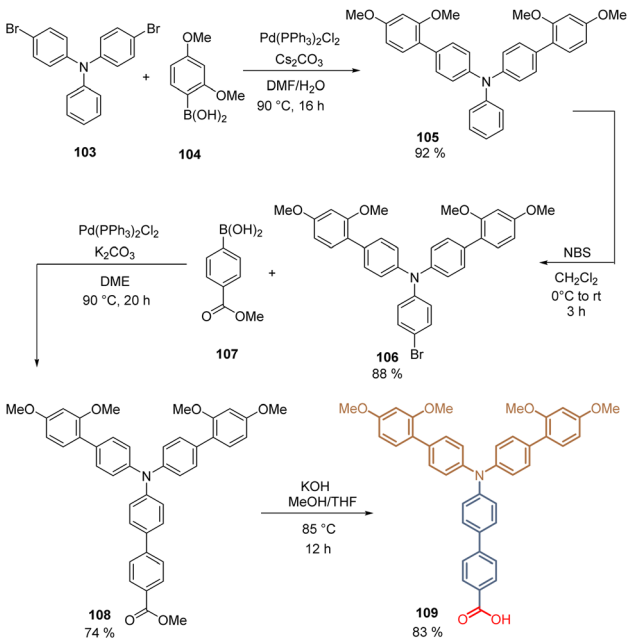

Scheme 12 Synthesis of derivative **109** introducing the donor dimethoxyphenyl fragment on the TPA moiety.

Further, we examined the role of the substitution pattern in the TPA fragment by modifying the positions of the methoxy substituents. Thus, disubstituted molecules: *ortho–para* **113a**, *ortho–meta* **113b**, and *meta–para* **113c** were prepared in a three-step synthetic route starting from 4-bromo-*N*-(4-bromophenyl)-*N*-phenyl aniline **103** that was formylated through the Vilsmeier–Haak reaction to furnish the carboxaldehyde **110**. This intermediate was then subjected to the Suzuki coupling with different disubstituted boronic acids **111a–c** to obtain compounds **112a–c** in good to excellent yields (85–90%). Finally, the oxidation with $KMnO_4$ furnished the desired compounds **113a–c** with the carboxylic acid as an anchoring group in moderate yields (Scheme 13).[97]

Depending on the substitution pattern, the work function and surface properties of the electrode changed, and following theoretical calculations, the *ortho–para* **113a** derivative gave the best results with a PCE = 19.8%. This is because the methoxy groups at *ortho–para* positions contributed to forming a well-ordered array during the SAM deposition, enhancing its stability and bonding on the metal oxide surface as well.

In 2020, it was reported the combination of the benzothiadiazole core with the TPA in the design of HTMs and SAMs for PSCs. This combination arose from previous experience on the synthesis of several metal-free dyes used in DSSCs following the strategy of the donor–acceptor backbone, where the benzothiadiazole core acted as a spacer and the 2-cyanoacetic acid as the anchoring group. The resulting dyes enhanced the intramolecular charge transfer, the J_{SC} values, and the solubility of the corresponding compounds in polar solvents. Thus, in the first approach, MeOTPA-boronic ester **114a** reacted with benzo[*c*][1,2,5]-thiadiazole carbaldehyde **115** *via* Suzuki coupling to give intermediate **116** in excellent yield (95%), the final Knoevenagel condensation with cyanoacetic acid afforded the HTM **117** in 75% yield allowing the formation of SAM on ITO to fabricate a PSCs device that displayed a PCE of 21.24% (V_{OC} = 1.13 V, J_{SC} = 22.25 mA cm^{-2}, FF = 84.8%) (Scheme 14).[98] The same research group explored the effect of different anchoring groups in the TPA-benzothiadiazole moiety. For that, from intermediate **116**, and employing rhodanine-3-propionic acid **118** as a nucleophile, the Knoevenagel reaction furnished the derivative **119** in 71% global yield for the fabrication of PSCs that showed a PCE of 19.65% (V_{OC} = 1.10 V, J_{SC} = 22.03 mA cm^{-2}, FF = 81.1%). The low performance of the rhodamine fragment as the anchoring group was attributed to the aggregation in the solid state of **119** due to the sp^3 hybridization of

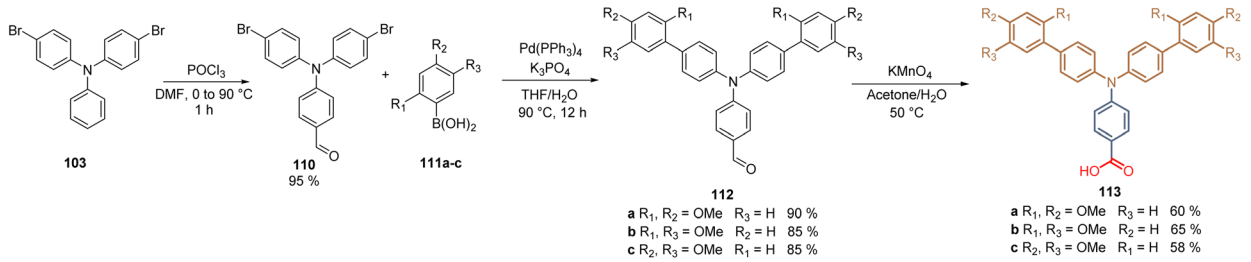

Scheme 13 Synthesis of molecules **113a–c** prepared to study the role of the substitution pattern in TPA-based SAMs in PSCs.

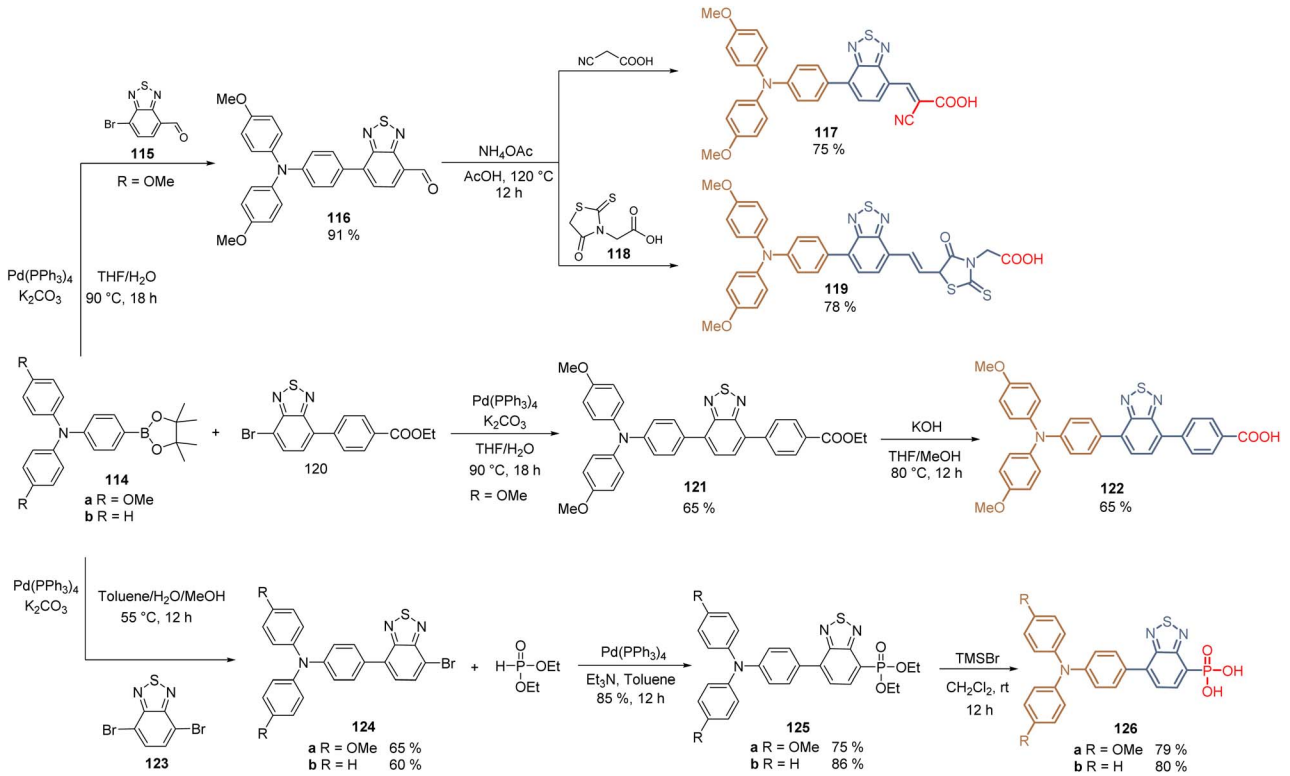

Scheme 14 Synthesis of TPA- TPA-benzothiadiazole HTMs for the fabrication of SAMs with different anchoring groups.

the carbon atom on this group, affecting the assembling of the molecules. While the preparation of **122** required the previous synthesis of **120** from commercially available reagents, and after the Suzuki coupling and hydrolysis, a TPA-benzothiadiazole derivative with the carboxylic acid **122** as an anchoring group was obtained in 21% global yield (Scheme 14). The PSC devices prepared with the SAM formed by **122** displayed a PCE of 20.58% ($V_{OC} = 1.12$ V, $J_{SC} = 22.76$ mA cm^{-2}, FF = 81.0%).[99]

Finally, the introduction of the phosphonic acid function as an anchoring group in the TPA-benzothiadiazole moiety was recently achieved through the stoichiometrically controlled Suzuki reaction between MeOTPA **114a** and TPA **114b** and dibromobenzothiadiazole **123**. The reaction gave the intermediates **124a an b** in moderate yields (60–65%), which were modified by the Michaelis–Becker reaction to furnish the phosphonates **125a and b** in good yields (75–86%). The corresponding ester functions were cleaved using TMSBr to obtain compounds **126a and b** (79–80%) (Scheme 14). The corresponding SAMs interacted with ITO through the oxygen of the anchoring group and the sulfur of the spacer group, forming a preferred "face-on" molecular orientation that reduced the hole injection barrier, constituting a new insight for SAMs. Interestingly, the devices fabricated with **126b** resulted to be more efficient (PCE of 23.24%, $V_{OC} = 1.14$ V, $J_{SC} = 24.83$ mA cm^{-2}, FF = 82.0%) than the ones with the **126a** (PCE of 21.52%, $V_{OC} = 1.10$ V, $J_{SC} = 24.70$ mA cm^{-2}, FF = 79.2%), that contained the methoxy donor groups in the TPA core.[100]

As a concluding remark, the molecules based on the TPA-benzothiadiazole moiety **117**, **119**, **122** and **126a and b**, show the beneficial effect of the benzothiadiazole core, where the planarity of this spacer group enhances the intermolecular stacking, while the sulfur atom can interact with under-coordinated Pb^{2+} ions *via* coordination bonds. Finally, passivation effects were also observed for molecule **126b** containing the phosphonic acid function as an anchoring group.

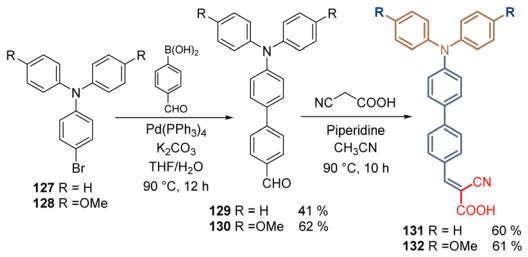

Scheme 15 Synthesis of electron-rich TPA derivatives **131** and **132** with conjugated spacer groups.

The same authors that reported the synthesis of carbazole-based molecules with conjugated spacer groups (See Scheme 9), studied the effect of the TPA moiety using two aromatic rings as a spacer group in combination with the cyanoacetic acid as an anchoring group. The synthesis of compounds **131** and **132** involved a traditional Suzuki coupling from the commercial TPA-Br derivatives **127** and **128**, followed by a Knoevenagel condensation to insert the corresponding anchoring group (Scheme 15).[88] Indeed, the performance of compound **132** in inverted PSCs was better than its related carbazole derivative **91** exhibiting a PCE = 22.53%, (*vs.* PCE = 20.66% of **91**), and enhanced stability under UV light.

Similar results have been obtained recently with a TPA derivative containing just one aromatic group as a spacer group and the cyanoacetic acid moiety as an anchoring group when the SAM is formed onto a NiO_x surface (PCE = 20.94%).[101]

Based on the synthetic concepts described in this section, we can conclude that the discovery of the next generation of molecules containing the triphenylamine core, and taking into account the excellent PCEs of TPA-based SAMs PSCs, efforts are required to achieve the facile and cost-effective synthetic routes. In addition, the commercial availability of building blocks containing TPA makes it easier to explore alternative donor moieties on the TPA core, and combinations with different spacers and anchoring groups.

Phenothiazine-SAMs

Phenothiazine derivatives have been extensively used in DSSCs as organic sensitizers.[102] However, during the last year this structure has been raised as one of the most promising materials for SAMs in PSCs.[103] Phenothiazine is a well-known electron-rich heterocyclic compound whose main properties are the presence of the electron-donating sulfur and nitrogen heteroatoms, and its nonplanar butterfly conformation, that prevents intermolecular aggregation, leading to efficient hole-transport capability.[104]

The optical, electrochemical, and photovoltaic properties of HTMs based on the phenothiazine core have inspired the design and synthesis of small molecules for SAMs. The first study was published in 2019 with the synthesis of a unique phenothiazine unit functionalized with TPA groups **135**. Using commercial phenothiazine **133** as the starting material, a bromination reaction was performed to selectively activate positions 3 and 7 and proceed with a Suzuki coupling to obtain the fragment **135** in good yield (65%), with both excellent hole-extraction/transportation fragments (Scheme 16).[105]

The same authors then reported the introduction of an alkyl chain at the 10-position of phenothiazine **135** and also decorated the terminal position of this chain with different anchoring groups: –COOH **137**, $-SO_3H$ **138**, and $-PO(OH)_2$ **139**.[106] These transformations were performed *via* a nucleophilic substitution reaction with the respective alkyl bromides under basic conditions. In general, compounds **136–139** were obtained in moderate to good yields (47–79%) using cheap and accessible starting materials (Scheme 17).

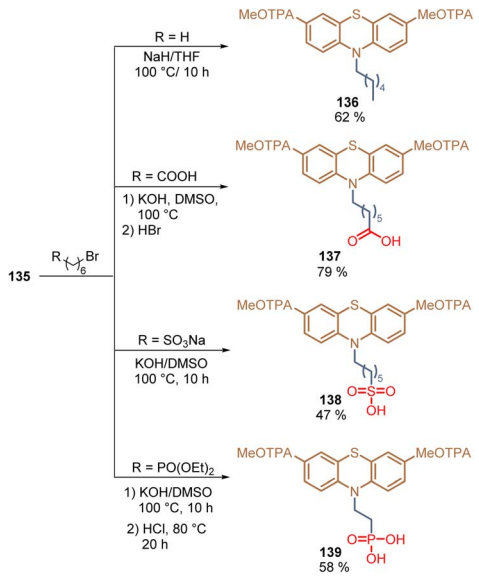

Scheme 17 Synthesis of phenothiazines with different anchoring groups: –H **136**, –COOH **137**, $-SO_3H$ **138**, and $-PO(OH)_2$ **139**.

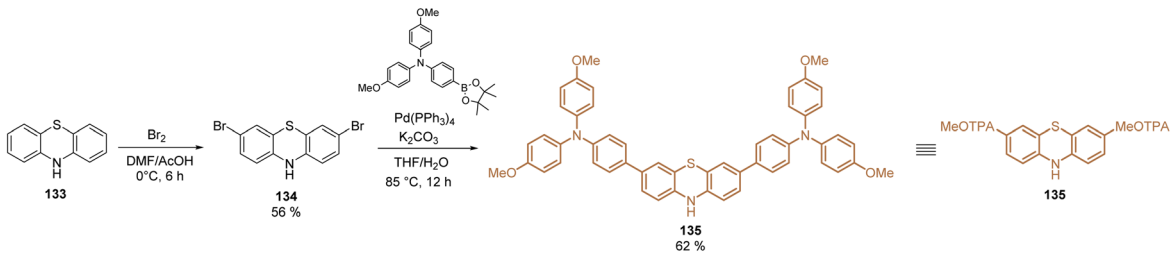

Scheme 16 Synthesis of phenothiazine **135** with TPA groups functionalized at positions 3 and 7.

Using compound **136**, without any anchoring group as a reference, the adsorption and layer formation of SAMs **137–139** on ITO substrates were studied for the fabrication of PSCs. Among these anchoring groups, the phosphonic acid functionality of **139** exhibited the strongest anchoring interaction giving the highest PCE (21.93%).

With the idea to reduce the molecular complexity compared with phenothiazine derivatives **136–139** and test the effect of electron-withdrawing groups in this core, bromide groups were included at positions 3 and 7 through a rapid and straightforward synthetic route. It started from phenothiazine **133** that was *N*-alkylated to give intermediate **140**, whose hydroxyl function was transformed into a terminal bromide group in **141** (Scheme 18). The tribromated derivative **142** was obtained after Br_2 treatment and the subsequent Arbuzov reaction followed by the cleavage of the ethyl groups furnished the dibromo phenothiazine **144** in 9% global yield.[107] The tailored SAM **144** was used in p-i-n PSCs, exhibiting a PCE = 22.44%, with FF = 82%, being one of the highest efficiencies reported for p-i-n PSCs.

The bulky sulfur atom present in the phenothiazine core helps to prevent the effective π–π stacking of molecules, facilitating their assembly and increasing the solubility of these derivatives in various organic solvents. So, based on these facts, the same research group reported the design and synthesis of two variants of **144** by replacing the S with oxygen and selenium in the head group of the phenothiazine core. To increase the global yields, another strategy was performed for the synthesis of these derivatives. The corresponding phenothiazine **133**, phenoxazine **133a**, and phenoselenazine **133b** were subjected to an acylation reaction to obtain derivatives **145** in good yields and with the terminal bromide already installed in the alkyl chain. The following reduction of the carbonyl function promoted by the borane–tetrahydrofuran complex afforded intermediates **141** in good yields, that were finally transformed using the same protocol as for **144** (bromination/Arbuzov/deprotection) (Scheme 19).[108]

Derivatives **144** formed a well-assembled layer providing an adequate interface with the perovskite layer to reduce the interfacial trap density and enhance the charge-carrier lifetime. Although the SAMs showed negligible differences in the device parameters, it was found that the interfacial interaction energies between the SAMs and the perovskite layer were strongly influenced by the polarizability of the heteroatoms present at the phenothiazine core, which increased in the order of Se > S > O. This was reflected on the PCE, being 144b-Se (22.73%) > 144-S (21.63%) > 144a-O (21.02%).

One of the main reasons why phenothiazine is captivating the interest of several research groups, besides the promising results obtained in PSC devices, is its low cost as a building block, which allows for the sustainable synthesis of stable HTMs with different tuneable photo- and electrochemical properties due to its well-known reactivity.

Thiophene-SAMs

Thiophene, and other related S-rich heterocyclic derivatives such as thienopyridine, thienothiophene, and bithiophene imide, have been used as π-type linkers in different HTMs. The flat, rigid, and good electron delocalized skeleton in the thiophene ring, plus the prolonged molecular conjugation and intermolecular S···S interactions, results in HTMs with good hole mobilities and conductivities for PSCs.[109]

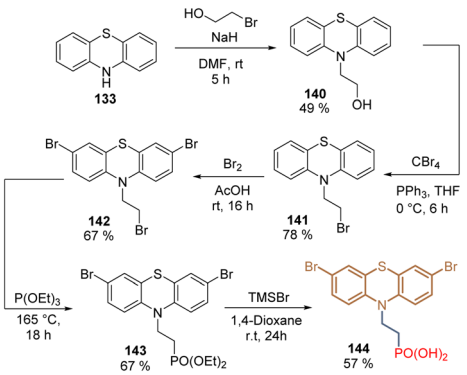

Scheme 18 Synthesis of phenothiazine **144** substituted with electron-withdrawing groups at positions 3 and 7.

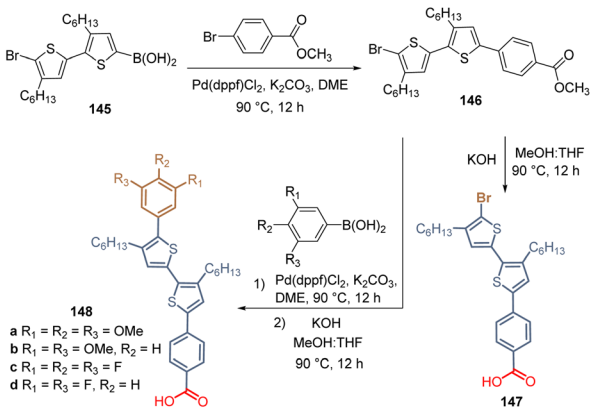

Scheme 20 First examples of bithiophene derivatives **147** and **148a–d** prepared to form SAMs in PSCs.

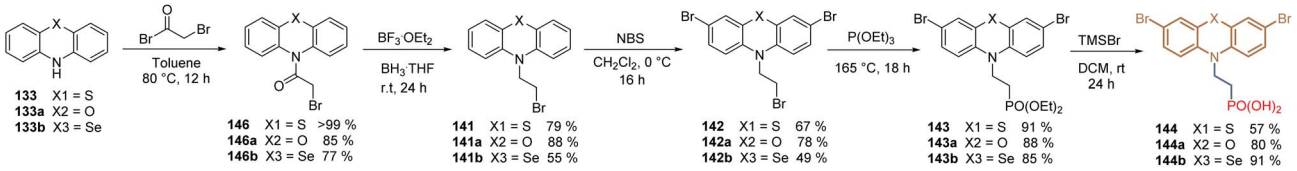

Scheme 19 Phenothiazines derivatives incorporating sulfur **144**, oxygen **144a** and selenium **144b** on the head group.

The first work in which thiophene rings were used as spacers was reported in 2020. It consisted of the synthesis of bithiophene derivative **147** after the Suzuki coupling followed by the corresponding hydrolysis to obtain the carboxylic acid function as an anchoring group (Scheme 20). Compound **147**, having the bromide atom as a functional group, formed a layer of SAM on the ITO electrode and the PSC device showed a PCE = 11.89% in a p-i-n type device configuration.[110]

The same authors then introduced a series of aromatic rings *via* Suzuki coupling at the brominated position of **146**, with different electron-donating (MeO–) and withdrawing (F–) characteristics, obtaining a series of derivatives **148**. Unfortunately, the yields are not reported in any of their works (Scheme 20). In this study, the highest PCE (12.03%) was achieved with the compound **148b**, substituted with two methoxy groups at positions 3 and 5. Later, they reported the introduction of TPA and carbazole moieties as a functional group in the structure of bithiophene **146** (Scheme 21). Thus, using the same synthetic approach, Suzuki coupling/hydrolysis, the series of derivatives **150a–c** were obtained and used in the fabrication of p-i-n type PSC devices.[111] Although the efficiency showed by these devices resulted to be slightly higher than for the ones prepared with compounds **147** and **148a–d**, the best PCE (13.71%) was achieved by compound **150b**, having the MeOTPA core as a functional group.

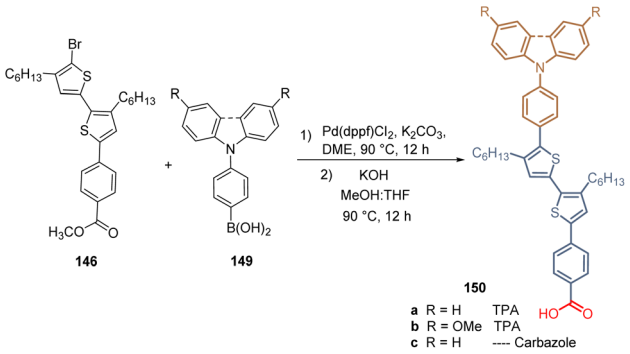

Scheme 21 Synthesis of bithiophene derivatives **150a–c** having the TPA and carbazole moieties as functional groups.

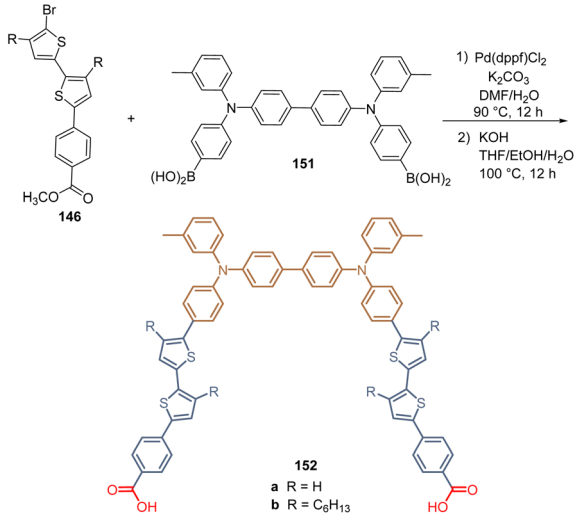

Scheme 22 Synthesis of the thiophene derivative **152** with two anchoring groups for the formation of bidentate SAM.

Finally, the same research group continued with their work by designing two molecules **152a and b** for the formation of bidentate SAMs by reacting the intermediates **146** with the TPA-diboronic acid derivative **151** under their standardized synthetic protocol (Scheme 22). Unfortunately, the efficiency did not exceed 13.12% for derivative **152a**, although this concept of two anchoring groups in the same molecular architecture would be interesting to obtain better SAMs. It was found that the presence of hexyl chains could create a steric hindrance that would affect the assembled process during the SAM formation.[112]

The layers of SAMs not only can be formed on metal oxide surfaces, as discussed in the sections above. The crystalline perovskite layer could also serve as a template for the ordered assembly of molecules containing the same elements as a SAM: anchoring, spacer, and functional groups. This approach was reported in 2021 where three molecules with one thiophene unit as a spacer group were prepared *via* Suzuki coupling/Knoevenagel condensation protocol starting from thiophene carboxaldehyde **153** and different boronic acids **154**. The respective intermediates **155** were then condensed with cyanoacetic acid and the desired molecules **156a–c** were obtained (Scheme 23). The reaction yields unfortunately were not reported although the dipole moment of these molecules was determined, being 11.33 D the highest one for the compound **156c** with the dimethylaminophenyl moiety as a functional group. The dipole moments play a key role in the preferential orientation of the assembled molecules on the perovskite surface. This is due because the functional group (which has the highest electron density) interacts with the undercoordinated Pb(II) of the perovskite, promoting the growth of a layer of SAMs on the top. As a result, the PSCs device using compound **156c**, with the highest dipole moment, exhibited a PCE of 21.4%.[113]

The works discussed in this section are focused exclusively on the use of thiophene as a spacer group. Besides compound

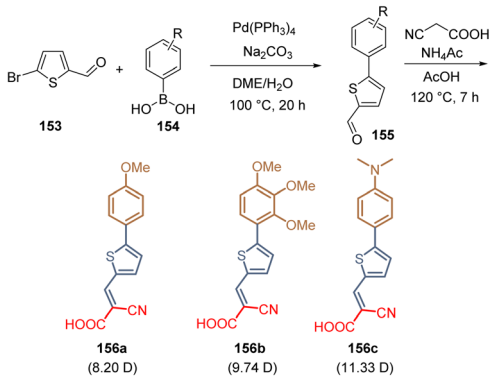

Scheme 23 Examples of molecules with one thiophene ring are a spacer group, a similar anchoring group, and different functional groups showing different dipole moments.

156c, the PSC devices fabricated with the other related molecules show poor efficiencies. However, S-rich heterocyclic compounds can be still applied in the design of SAMs, because they form part of efficient HTMs. In the case of small molecules designed as SAMs, these electron-rich systems should be used as a functional group instead of a spacer to take advantage of the well-known interaction and passivation of the Pb by the heterocyclic sulfur atoms.

Uncommon-SAMs

In the last section, we will cover the application of a series of SAMs that do not belong to any of the families of compounds already described, thus they are classified as "uncommon" SAMs. These molecules possess a unique structure keeping at the same time the requirements for SAMs, prepared through elegant synthetic approaches.

In 2019, the naphthalimide core was introduced as a spacer and as a functional group. Thus, exploiting the reactivity of naphthalic anhydride **157**, the electron-rich piperidine fragment was incorporated through nucleophilic aromatic substitution to give **158** and, after the condensation with β-alanine tertbutyl ester, **159** was hydrolysed into **160** with a global yield of 27% (3 steps). On the other hand, compound **163**, with the 4-trifluoromethylphenyl electron withdrawing fragment, was prepared similarly but performing first the condensation reaction to furnish **161**, then the Suzuki coupling and finishing with the hydrolysis to give **163** 52% global yield (3 steps) (Scheme 24). In both compounds **160** and **163**, the naphthalimide core acted as a spacer group, however, the performance did not exceed 6% (**163**, PCE = 5.66%). In contrast, when the naphthalimide core was used as a functional group, such as in **165**, the PCE increased up to 14.92%. This molecule was prepared from the naphthalenetetracarboxylic acid anhydride **164** to obtain the bidentade molecule with a 90% yield (Scheme 24).

The increase in the PCE for SAM **165** is due to the planar interaction between the functional group and the perovskite layer that enhances the electron extraction.[114]

Ionic liquids have also been applied as SAMs due to the reactivity of hydroxyl groups towards metal oxide surfaces and the high conductivity, wide electrochemical window, and excellent thermal stability. The hydroxyethyl functionalized imidazolium iodide **169** was obtained as a solid at room temperature in high yield through the Ullman coupling between bromide **166** and imidazole **167**, followed by the metathesis with 2-iodoethanol (Scheme 25). The layer of SAMs formed by **169** onto the FTO substrate lowered the work function of the conductive electrode and increased the interfacial electron extraction, retarding at the same time the charge recombination, resulting in a PCE = 17.31%. This work demonstrated the potential of ionic liquids as SAMs to reduce the number of layers in the devices and the associated fabrication costs.[115]

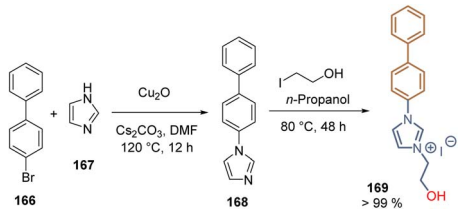

Scheme 25 Preparation of functionalized ionic liquid **169** for the deposition of SAMs on the FTO surface.

In 2020, our group reported what has been so far the only organometallic compound used to form a layer of SAMs for PSCs. Phthalocyanine **171** is efficiently attached to metal oxide surfaces such as ITO and gives promising results when applied in DSSCs. We thus reported the direct transformation of the hydroxyl methyl phthalocyanine **170** into its corresponding carboxyl derivative **171** catalysed by ZnO in high yield (96%) (Scheme 26). Traditionally, this transformation requires strong oxidants and harsh conditions that may provoke the demetallation of **170**, furnishing a complex mixture of crude materials that is difficult to purify. Under our reaction conditions, **171** was obtained in a clean protocol and tested in PSCs as a SAM, exhibiting a PCE of 13.11% and establishing that the open-circuit voltage and overall efficiency are correlated to the differences in the energy levels rather than recombination kinetics.[116]

Besides some commercial molecules, all the synthetic molecules used to form SAMs contain tertiary amines as functional groups. However, primary amines, especially the protonated amines groups, could also passivate the perovskite layer and create a 2D perovskite sublayer between the SAM and

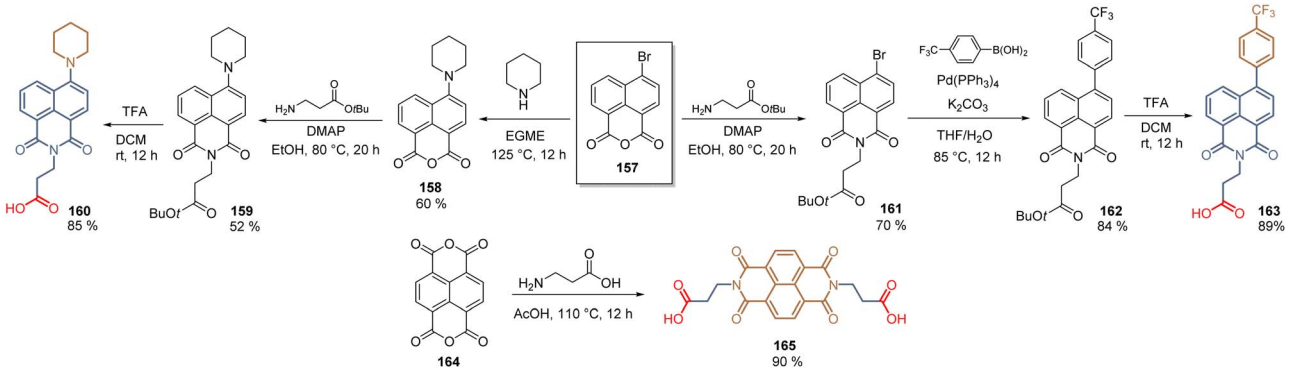

Scheme 24 Synthesis of naphthalimide derivatives **160**, **163**, and **165** for the formation of SAMs in n-i-p perovskite solar cells.

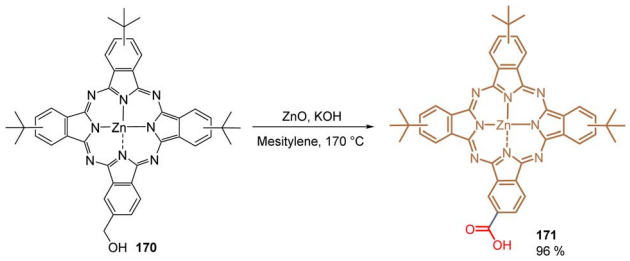

Scheme 26 Synthesis of the carboxylated Zn-phthalocyanine derivative **171**.

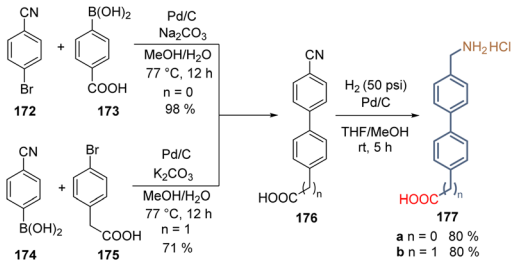

Scheme 27 Synthesis of molecules **177a and b** bearing a methylene group to induce flexibility on the layer of SAMs formed on the ZnO surface.

the active 3D-based perovskite layer. Bearing this idea in mind, two molecules with protonated amino groups as functional groups were designed and prepared easily from commercial and cheap precursors. The molecules, **177a** and **177b** are made of the biphenyl moiety as a spacer group to promote the self-assemble process and ensure conductivity, and methylene groups to add flexibility to the SAM, facilitating the bonding to the surface and the interaction with the perovskite layer. Starting from benzonitrile **172** and boronic acid **173**, intermediate **176** with the anchoring group directly connected to the spacer group was obtained and subjected to a nitrile reduction to afford the first compound **177a** in good yield (Scheme 27). On the other side, exchanging the functionalities in precursors **174** and **175**, product **177b** having the methylene group on both sides of the molecule was prepared in good yield as well (Scheme 27). It is worth highlighting that the Suzuki couplings reported in this study were performed under mild conditions and using the more accessible and stable Pd/C catalyst instead of the traditional $Pd(PPh_3)_4$ approach, opening the door to its implementation in this kind of transformation.

The deposition of SAMs formed by **177a and b** was done onto the ZnO surface and, despite the modest PCE of 8.8% for **177b**, this work demonstrated that the free rotation of SAMs, promoted by the $-CH_2-$ groups, contributes to the spatial adaptation and bonding to the metal surface. Moreover, it also

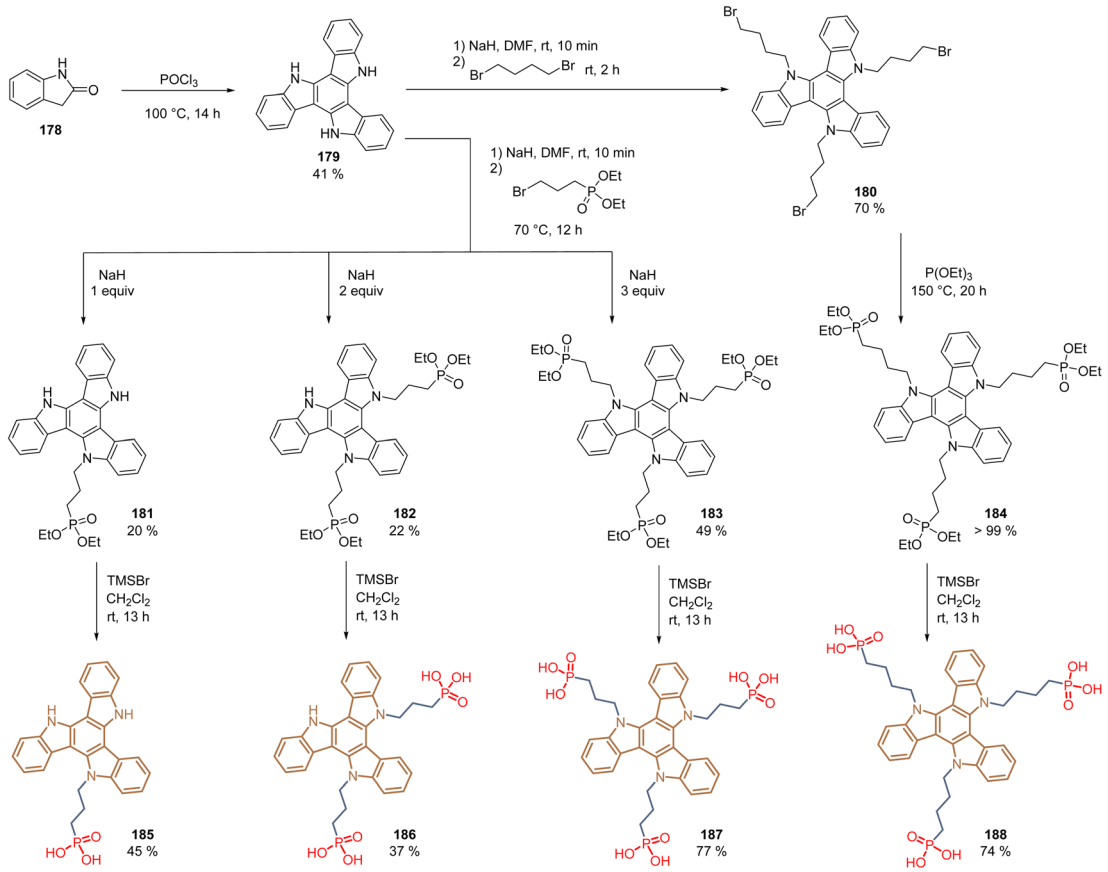

Scheme 28 Synthesis of the triazatruxene derivatives **185–188** for the formation of multipodal SAMs in PSCs.

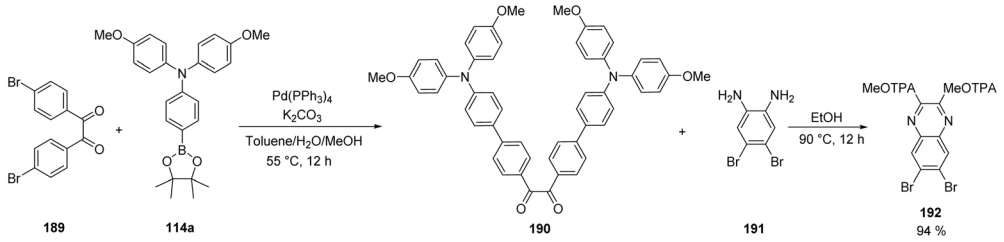

Scheme 29 Preparation of quinoxaline **192** containing two MeOTAP fragments as functional groups *via* condensation reaction.

affects the interaction and adaptation of the perovskite network.[117]

The concept of molecules having two anchoring groups resulted attractive in studies with molecules such as **49**, **152**, and **165**. However, this approach was extended recently to molecules with multiple anchoring sites, creating tridentate SAMs. The bonding of a molecule to a metal surface through one anchoring group usually orients the π-plane of the functional group perpendicular to the metal surface and the perovskite layer. Through the multipodal strategy, the π-conjugated backbone of the functional group is face-on orientated to the substrate and the perovskite surface, resulting in an efficient orbital overlap that suppresses the interfacial recombination and enhances the hole extraction. Under this approach, the structure of triazatruxene **179**, prepared from 2-oxindole **178** in moderate yield, was functionalized *via* *N*-alkylation to obtain derivatives **180**, substituted with three C_4-alkyl chains, and intermediates **181–183**, that depending on the number of equivalents of NaH employed, generated the corresponding the mono-, di- and trialkylated products with C_3-alkyl chains (Scheme 28). In the case of derivatives **181–183**, simple hydrolysis using TMSBr gave the desired monopodal **185**, dipodal **186**, and tripodal **187** compounds with the phosphonic acid function as anchoring groups. The derivative **180** was first subjected to the Arbuzov reaction followed by the cleavage of the ethyl groups to obtain the corresponding tripodal

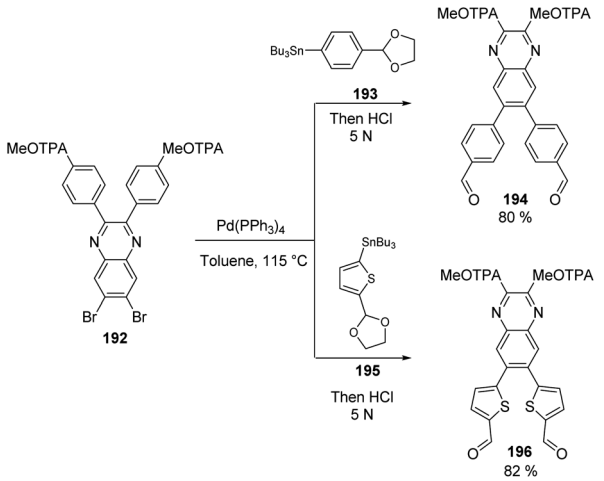

Scheme 30 Synthetic route for the construction of the spacer group around the quinoxaline core in derivatives **194** and **196**.

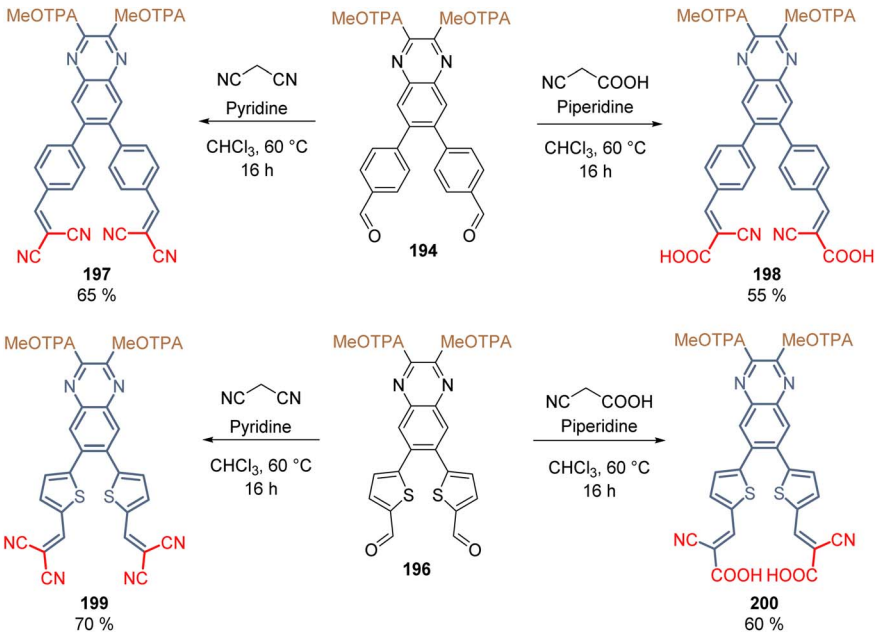

Scheme 31 Synthesis of the X-shape derivatives **197–200** with the MeOTAP donor group and nitrile functionalities as anchoring groups.

compound **188** substituted with three C_4-alkyl chains and the phosphonic acids as anchoring groups (Scheme 28).

In general, the reactions proceeded well, except for derivatives **181** and **182**, where despite controlling the equivalents of NaH, side reaction occurred, generating by-products that hindered the purification processes.

Compounds **185–188** form a layer of SAMs on both ITO and FTO surfaces *via* mono-, bi- and tridentate binding modes. The PSC devices fabricated with these molecules gave the following PCEs: **185** (21.1%), **186** (22.2%), **187** (23.0%), and **188** (22,1%), demonstrating the effectiveness of the tripodal mode in comparison to mono-and dipodal modes. Moreover, it was shown that the spacer length of 3-carbon atoms is more adequate to achieve a face-on orientation, without affecting the charge transport, in comparison with the 4-carbon atom spacer group.[118]

Quinoxalines are a class of heterocyclic compounds in which two nitrogen atoms replace two carbons in the ring of naphthalene. These moderate electron-withdrawing cores have a low synthetic cost, whereas the pyrazine heterocycle facilitates chemical modification giving the possibility of obtaining molecules with different shapes. Thus, a series of quinoxalines **197–200** were prepared through various synthetic steps pursuing the design of novel compounds with a quinoxaline core in the spacer and exhibiting an X-shape, where the four reactive sites are symmetrically substituted.

One of the most used protocols for the synthesis of quinoxalines is the condensation of *ortho*-diamines with 1,2-diketones. This strategy was implemented using the modified diketone **190**, in which the donor MeOTAP fragments were introduced *via* Suzuki coupling between substrate **189** and boronic ester **114a**. Then, the condensation of **190** with diamine **191** successfully afforded intermediate **192** in excellent yield, containing two MeOTAP fragments as functional groups and the quinoxaline core functionalized with two bromides to be transformed in the next steps (Scheme 29).

The intermediate **192** was then used as a precursor in the Stille coupling reaction with different organostannanes, **193** and **195**, to obtain the derivatives **194** and **196** in good yields (Scheme 30). With this transformation, the spacer groups were completed, being the quinoxaline-phenyl core the one for **194** and the quinoxaline-thiophene core for **196**. The aldehyde functions on precursors **193** and **195** were protected as acetals due to their sensitivity under the Stille reaction conditions, but a routine acidification during the work-up process restored these functional groups needed in the further steps to insert the anchoring groups.

Finally, the two anchoring groups (CN/CN and CN/COOH) were introduced in each derivative **194** and **196** through the Knoevenagel condensation (Scheme 31). For the insertion of the CN/CN anchoring group, the reactions were performed using malononitrile and pyridine as a base, while the insertion of CN/COOH was achieved with cyanoacrylic acid and piperidine as a base (Scheme 31). Products **197–200** were obtained in moderate yields and, according to their substitution pattern, they exhibited a well-defined X-shape around the quinoxaline spacer group.

The layer of SAMs was formed on ITO using molecules **197–200** and Sn-based PSCs were fabricated with these materials, obtaining acceptable efficiencies. The PCE values were 6.1% (**197**), 7.1% (**198**), 8.0% (**199**) and 8.3% (**200**), where the derivative with thiophene π-extended conjugation and the cyanoacetic moiety as anchoring group exhibited the highest hole extraction rates, greatest hole mobilities, and slowest charge

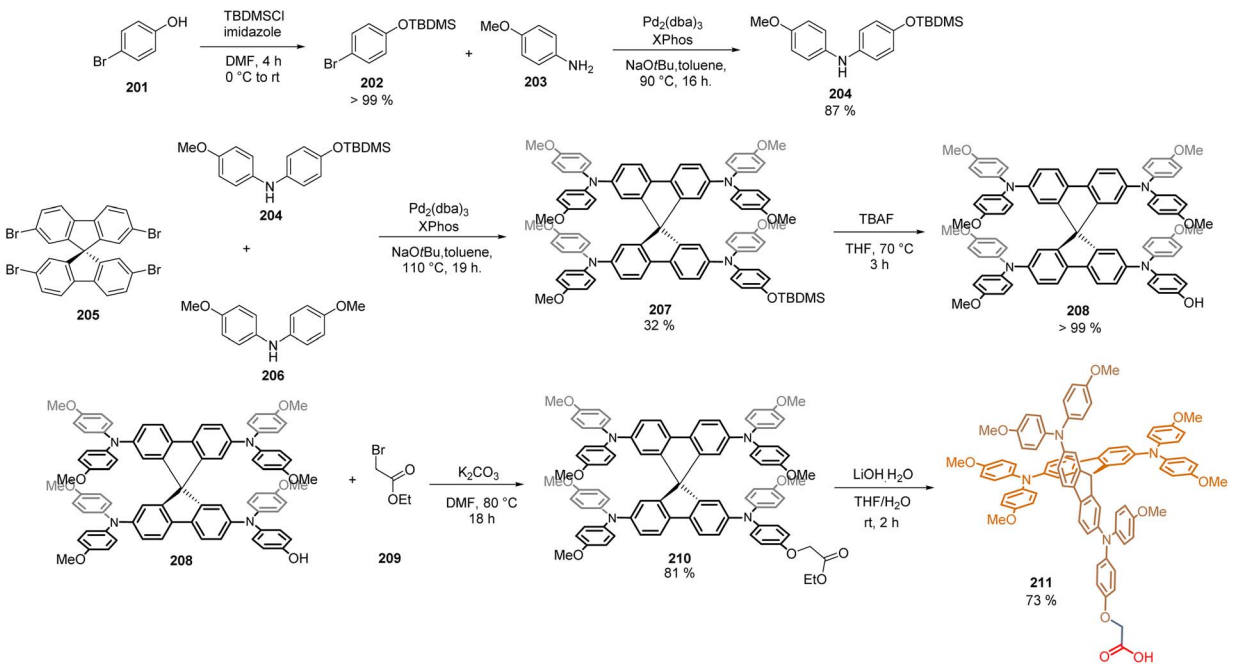

Scheme 32 Synthesis of the spiro OMeTAD derivative **211**.

recombination, resulting in the best device performance ever reported in Sn-PSCs.[119]

The commercially available Spiro-MeOTAD is one of the most studied HTMs in high-efficiency PSCs, achieving a record PCE = 25.8% in the n-i-p configuration. Inspired by this, our group recently reported the synthesis of a Spiro-MeOTAD derivative featuring a carboxylic acid unit to act as an anchoring group. The synthesis of this Spiro-acid compound **210** required the preparation of intermediate **208**, in which one of its methoxy groups in the TAP core is replaced by a hydroxyl group. Thus, bromo phenol **201** was efficiently protected using *tert*-butyldimethylsilyl chloride as a protecting group. Later, **202** was coupled *via* Buchwald–Hartwig reaction with anisidine **203**, to yield diphenylamine mono-methoxylated **204** (87%) (Scheme 32). Then, the 2,2′,7,7′-tetrabromo-9,9′-spirobifluorene **205** was subjected to another Buchwald–Hartwig tetra-amination reaction using the intermediate **204** and the commercial bis(4-methoxyphenyl)amine **206**. At this point, the crucial step of the synthetic protocol was the isolation and purification of the desired product **207**, since during this reaction, a complex mixture of by-products was formed. However, once the product **207** (32%) was obtained and characterized, the *O*-deprotection furnished the hydroxyl compound **208** in quantitative yield and was then coupled, through a Williamson ether reaction with the commercially available ethyl bromoacetate **209**, to obtain the ester **210**. Then, it underwent a saponification reaction with lithium hydroxide to give Spiro-acid **211** in 16% overall yield (Scheme 32).

The SAM **211** was deposited on the ITO surface in the p-i-n configuration of the PSC giving PCE = 18.15%. The devices showed ultralow energy loss and a remarkable fill factor (82%), paving the way for the application of modified structures of Spiro-MeOTAD at the hole transport layer without the need for chemical dopants.[120]

Conclusions

The number of "small molecules" that can be potentially synthesised and used as SAMs are endless. Yet, the understanding of the effects of such molecules on the perovskite material remains elusive and needs further investigation. The pursuit of higher efficiencies in perovskite solar cells will, definitively, make use of SAMs at the interface either in tandem solar cells with silicon films or with organic semiconductor thin films. A myriad of new molecules has been described and for sure this perspective will provide a handy tool to quickly read what has been done so far in the scientific literature about SAMs for PSC.

In this respect, we have presented a comprehensive overview of the rational design and synthesis of all the molecules used as SAMs in PSCs, from the original seminal works using commercial molecules to the most complex structures prepared so far in this field. Despite the efforts made to prepare these molecules and fabricate efficient and stable perovskite devices, several key challenges remain for organic chemists, who need to focus their efforts on the design of new molecules containing the concepts described in this review, selecting the best combination of anchoring, spacer, and functional groups, also targeting facile and cost-effective protocols for the synthesis of these molecules to accelerate the commercial and industrial generation of solar energy with perovskite solar cells. A true challenge will be to design molecules that, from one side, improve charge transfer from the perovskite to the contacts and, from the other side, modify the perovskite surface to vastly enhance the perovskite stability and avoid leaking of lead from the crystalline structure. Of course, SAMs that achieve similar effects on Sn-based perovskite films are the other challenges scientists face for the next decade.

Author contributions

All authors contributed to the writing and revision of the manuscript, and have approved the final version of this review article.

Conflicts of interest

There are no conflicts to declare.

Acknowledgements

The authors acknowledge financial support from Spanish Government and AGAUR (Ministerio de Ciencia e Innovacion Severo Ochoa Grant MCIN/AEI/10.13039/501100011033 (CEX2019-000925-S), PID2019-109389RB-I00, PID2022-139866NB-I00 funded by MCIN/AEI/10.13039/501100011033/FEDER, UE and 2021 SGR 01261, respectively). C.P. thanks the European Union (Horizon 2020 Marie Skłodowska-Curie COFUND grant agreement no. 801474) D. A. G. acknowledges financial support from the MINECO predoctoral fellowship (BES-2017-082439). E. P. also acknowledges ICIQ, CERCA, and ICREA for financial support.

References

1 J. Y. Kim, J.-W. Lee, H. S. Jung, H. Shin and N.-G. Park, *Chem. Rev.*, 2020, **120**, 7867–7918.
2 Best Research-Cell Efficiency Chart, **https://www.nrel.gov/pv/cell-efficiency.html**, accessed: May 2023.
3 R. Wang, M. Mujahid, Y. Duan, Z.-K. Wang, J. Xue and Y. Yang, *Adv. Funct. Mater.*, 2019, **29**, 1808843.
4 H. Li and W. Zhang, *Chem. Rev.*, 2020, **120**, 9835–9950.
5 V. Romano, A. Agresti, R. Verduci and G. D'Angelo, *ACS Energy Lett.*, 2022, **7**, 2490–2514.
6 E. Aktas, N. Rajamanickam, J. Pascual, S. Hu, M. H. Aldamasy, D.-D. Girolamo, W. Li, G. Nasti, E. Martínez-Ferrero, A. Wakamiya, E. Palomares and A. Abate, *Commun. Mater.*, 2022, **3**, 104.
7 W. Chi, S. K. Banerjee, K. G. D. I. Jayawardena, S. Ravi P. Silva and S. Seok, *ACS Energy Lett.*, 2023, **8**, 1535–1550.
8 C. McDonald, C. Ni, P. Maguire, P. Connor, J. T. S. Irvine, D. Mariotti and V. Svrcek, *Nanomaterials*, 2019, **9**, 1481.
9 V. M. Le Corre, M. Stolterfoht, L. Perdigón Toro, M. Feuerstein, C. Wolff, L. Gil-Escrig, H. J. Bolink,

D. Neher and L. J. Anton Koster, *ACS Appl. Energy Mater.*, 2019, **2**, 6280–6287.
10 S. Foo, M. Thambidurai, P. S. Kumar, R. Yuvakkumar, Y. Huang and C. Dang, *Int. J. Energy Res.*, 2022, **46**, 21441–21451.
11 J. J. Yoo, G. Seo, M. R. Chua, T. G. Park, Y. Lu, F. Rotermund, Y.-K. Kim, C. S. Moon, N. J. Jeon, J.-P. Correa-Baena, V. Bulović, S. S. Shin, M. G. Bawendi and J. Seo, *Nature*, 2021, **590**, 587–593.
12 X. Lin, D. Cui, X. Luo, C. Zhang, Q. Han, Y. Wang and L. Han, *Energy Environ. Sci.*, 2020, **13**, 3823–3847.
13 (*a*) X. Zheng, Y. Hou, C. Bao, J. Yin, F. Yuan, Z. Huang, K. Song, J. Liu, J. Troughton, N. Gasparini, C. Zhou, Y. Lin, D.-J. Xue, B. Chen, A. K. Johnston, N. Wei, M. N. Hedhili, M. Wei, A. Y. Alsalloum, P. Maity, B. Turedi, C. Yang, D. Baran, T. D. Anthopoulos, Y. Han, Z.-H. Lu, O. F. Mohammed, F. Gao, E. H. Sargent and O. M. Bakr, *Nat. Energy*, 2020, **5**, 131–140; (*b*) B. Chen, P. N. Rudd, S. Yang, Y. Yuanc and J. Huang, *Chem. Soc. Rev.*, 2019, **48**, 3842–3867; (*c*) P. Roy, A. Ghosh, F. Barclay, A. Khare and E. Cuce, *Coatings*, 2022, **12**, 1089; (*d*) Z. Guo, A. K. Jena, G. M. Kim and T. Miyasaka, *Energy Environ. Sci.*, 2022, **15**, 3171–3222.
14 Y. Shao, Z. Xiao, C. Bi, Y. Yuan and J. Huang, *Nat. Commun.*, 2014, **5**, 5784.
15 M. Dkhili, G. Lucarelli, F. De Rossi, B. Taheri, K. Hammedi, H. Ezzaouia, F. Brunetti and T. M. Brown, *ACS Appl. Energy Mater.*, 2022, **5**, 4096–4107.
16 K. Mahmood, S. Sarwar and M. T. Mehran, *RSC Adv.*, 2017, **7**, 17044.
17 X. Zheng, B. Chen, J. Dai, Y. Fang, Y. Bai, Y. Lin, H. Wei, X. C. Zeng and J. Huang, *Nat. Energy*, 2017, **2**, 17102.
18 W.-Y. Chen, L.-L. Deng, S.-M. Dai, X. Wang, C.-B. Tian, X.-X. Zhan, S.-Y. Xie, R.-B. Huang and L.-S. Zheng, *J. Mater. Chem. A*, 2015, **3**, 19353–19359.
19 H. Zhang, H. Wang, H. Zhu, C.-C. Chueh, W. Chen, S. Yang and A. K.-Y. Jen, *Adv. Energy Mater.*, 2018, **8**, 1702762.
20 K. C. Wang, J. Y. Jeng, P. S. Shen, Y. C. Chang, E. W. Diau, C. H. Tsai, T. Y. Chao, H. C. Hsu, P. Y. Lin, P. Chen, T. F. Guo and T. C. Wen, *Sci. Rep.*, 2014, **4**, 4756.
21 M. Stolterfoht, C. M. Wolff, J. A. Márquez, S. Zhang, C. J. Hages, D. Rothhardt, S. Albrecht, P. L. Burn, P. Meredith, T. Unold and D. Neher, *Nat. Energy*, 2018, **3**, 847.
22 J. S. Yeo, R. Kang, S. Lee, Y. J. Jeon, N. Myoung, C. L. Lee, D. Y. Kim, J. M. Yun, Y. H. Seo, S. S. Kim and S. I. Na, *Nano Energy*, 2015, **12**, 96.
23 X. Sun, Z. Zhu and Z. Li, *Front. Optoelectron.*, 2022, **15**, 46.
24 S. Li, Y. L. Cao, W. H. Li and Z. S. Bo, *Rare Met.*, 2021, **40**, 2712.
25 X. Yin, Z. Song, Z. Li and W. Tang, *Energy Environ. Sci.*, 2020, **13**, 4057.
26 P. Mahajan, B. Padha, S. Verma, V. Gupta, R. Datt, W. C. Tsoi, S. Satapathi and S. Arya, *J. Energy Chem.*, 2022, **68**, 330.
27 Y. Wang, L. Duan, M. Zhang, Z. Hameiri, X. Liu, Y. Bai and X. Hao, *Sol. RRL*, 2022, **6**, 2200234.
28 P. Murugan, T. Hu, X. Hu and Y. Chen, *J. Mater. Chem. A*, 2022, **10**, 5044.
29 W. C. Bigelow, D. L. Pickett and W. A. Zisman, *J. Colloid Sci.*, 1946, **1**, 513.
30 K. Wojciechowski, S. D. Stranks, A. Abate, G. Sadoughi, A. Sadhanala, N. Kopidakis, G. Rumbles, C. Z. Li, R. H. Friend, A. K. Y. Jen and H. J. Snaith, *ACS Nano*, 2014, **8**, 12701.
31 S. K. Hau, H. L. Yip, O. Acton, N. S. Baek, H. Ma and A. K. Y. Jen, *J. Mater. Chem.*, 2008, **18**, 5113.
32 S. K. Hau, Y. J. Cheng, H. L. Yip, Y. Zhang, H. Ma and A. K. Y. Jen, *ACS Appl. Mater. Interfaces*, 2010, **2**, 1892.
33 A. Abrusci, S. D. Stranks, P. Docampo, H. L. Yip, A. K. Y. Jen and H. J. Snaith, *Nano Lett.*, 2013, **13**, 3124.
34 A. Ulman, *Chem. Rev.*, 1996, **96**, 1533.
35 M. Singh, N. Kaur and E. Comini, *J. Mater. Chem. C*, 2020, **8**, 3938.
36 Y. Wang, Q. Liao, J. Chen, W. Huang, X. Zhuang, Y. Tang, B. Li, X. Yao, X. Feng, X. Zhang, M. Su, Z. He, T. J. Marks, A. Facchetti and X. Guo, *J. Am. Chem. Soc.*, 2020, **142**, 16632.
37 T. Bauer, T. Schmaltz, T. Lenz, M. Halik, B. Meyer and T. Clark, *ACS Appl. Mater. Interfaces*, 2013, **5**, 6073.
38 F. Ali, C. Roldán Carmona, M. Sohail and M. Khaja Nazeeruddin, *Adv. Energy Mater.*, 2020, **10**, 2002989.
39 S. Y. Kim, S. J. Cho, S. E. Byeon, X. He and H. J. Yoon, *Adv. Energy Mater.*, 2020, **10**, 2002606.
40 J. Hu, W. Fu, X. Yang and H. Chen, *J. Polym. Sci.*, 2022, **60**, 2175.
41 S. Wang, H. Guo and Y. Wu, *Mater. Futures*, 2023, **2**, 012105.
42 C. Ganzorig, K. J. Kwak, K. Yagi and M. Fujihira, *Appl. Phys. Lett.*, 2001, **79**, 272.
43 J. V. Passarelli, D. J. Fairfield, N. A. Sather, M. P. Hendricks, H. Sai, C. L. Stern and S. I. Stupp, *J. Am. Chem. Soc.*, 2018, **140**, 7313.
44 E. Arkan, E. Yalcin, M. Unal, M. Z. Yigit Arkan, M. Can, C. Tozlu and S. Demic, *Mater. Chem. Phys.*, 2020, **254**, 123435.
45 L. Liu, A. Mei, T. Liu, P. Jiang, Y. Sheng, L. Zhang and H. Han, *J. Am. Chem. Soc.*, 2015, **137**, 1790.
46 L. Zuo, Z. Gu, T. Ye, W. Fu, G. Wu, H. Li and H. Chen, *J. Am. Chem. Soc.*, 2015, **137**, 2674.
47 L. Liu, A. Mei, T. Liu, P. Jiang, Y. Sheng, L. Zhang and H. Han, *Nano Lett.*, 2017, **17**, 269.
48 Q. Wang, C. C. Chueh, T. Zhao, J. Cheng, M. Eslamian, W. C. H. Choy and A. K.-Y. Jen, *ChemSusChem*, 2017, **10**, 3794.
49 D. A. Kara, K. Kara, G. Oylumluoglu, M. Zeliha Yigit, M. Can, J. J. Kim, E. K. Burnett, L. Gonzalez Arellano, S. Buyukcelebi, F. Ozel, O. Usluer, A. L. Briseno and M. Kus, *ACS Appl. Mater. Interfaces*, 2018, **10**, 30000.
50 G. Tumen-Ulzii, T. Matsushima, D. Klotz, M. R. Leyden, P. Wang, C. Qin, J. W. Lee, S. J. Lee, Y. Yang and C. Adachi, *Commun. Mater.*, 2020, **1**, 31.
51 Ç. Kırbıyık, T. Yılmaz Alıç and M. Kuş, *Microelectron. Eng.*, 2020, **231**, 111394.
52 T. Zhu, J. Su, F. Labat, I. Ciofini and T. Pauporté, *ACS Appl. Mater. Interfaces*, 2020, **12**, 744.

53 C. M. Wolff, L. Canil, C. Rehermann, N. Ngoc Linh, F. Zu, M. Ralaiarisoa, P. Caprioglio, L. Fiedler, M. Stolterfoht, S. Kogikoski, Jr., l. Bald, N. Koch, E. L. Unger, T. Dittrich, A. Abate and D. Neher, *ACS Nano*, 2020, **14**, 1445.
54 H. Shu, J. Xia, H. Yang, J. Luo, Z. Wan, H. Ashraf Malik, F. Han, X. Yao and C. Jia, *ACS Sustainable Chem. Eng.*, 2020, **8**, 10859.
55 C. Y. Chang, H. H. Huang, H. Tsai, S. L. Lin, P. H. Liu, W. Chen, F. C. Hsu, W. Nie, Y. F. Chen and L. Wang, *Adv. Sci.*, 2021, **8**, 2002718.
56 Ç. K. Kurukavak, T. Yılmaz, A. Büyükbekar and M. Kus, *Opt. Mater.*, 2021, **112**, 110783.
57 N. Singh and Y. T. Tao, *Nano Sel.*, 2021, **2**, 2390.
58 Y. Shi, H. Zhang, X. Tong, X. Hou, F. Li, Y. Du, S. Wang, Q. Zhang, P. Liu and X. Zhao, *Sol. RRL*, 2021, **5**, 2100128.
59 H. Dong, G. Shen, Z. Lin, Q. Cai, Y. Li, X. Xu, W. Zhang and C. Mu, *ChemNanoMat*, 2022, **8**, e202100475.
60 J. Zhang, J. Yang, R. Dai, W. Sheng, Y. Su, Y. Zhong, X. Li, L. Tan and Y. Chen, *Adv. Energy Mater.*, 2022, **12**, 2103674.
61 L. Liu, Y. Yang, M. Du, Y. Cao, X. Ren, L. Zhang, H. Wang, S. Zhao, K. Wang and S. Liu, *Adv. Energy Mater.*, 2023, **13**, 2202802.
62 Z. Chen, Y. Li, Z. Liu, J. Shi, B. Yu, S. Tan, Y. Cui, C. Tan, F. Tian, H. Wu, Y. Luo, D. Li and Q. Meng, *Adv. Energy Mater.*, 2023, **13**, 2202799.
63 T. Yang, W. Zhao, X. Liu and S. Liu, *Adv. Energy Mater.*, 2023, **13**, 2204192.
64 H. Zheng, F. Zhang, N. Zhou, M. Sun, X. Li, Y. Xiao and S. Wang, *Org. Electron.*, 2018, **56**, 89.
65 D. Bobb Semple, L. Zeng, I. Cordova, D. S. Bergsman, D. Nordlund and S. F. Bent, *Langmuir*, 2020, **36**, 12849.
66 S. K. Hau, Y. J. Cheng, H. Yip, Y. Zhang, H. Ma and A. K. Y. Jen, *ACS Appl. Mater. Interfaces*, 2010, **2**, 1892.
67 K. Wojciechowski, S. D. Stranks, A. Abate, G. Sadoughi, A. Sadhanala, N. Kopidakis, G. Rumbles, C. Z. Li, R. H. Friend, A. K. Y. Jen and H. J. Snaith, *ACS Nano*, 2014, **8**, 12701.
68 E. Aydin, J. Liu, E. Ugur, R. Azmi, G. T. Harrison, Y. Hou, B. Chen, S. Zhumagali, M. De Bastiani, M. Wang, W. Raja, T. G. Allen, A. ur Rehman, A. S. Subbiah, M. Babics, A. Babayigit, F. H. Isikgor, K. Wang, E. Van Kerschaver, L. Tsetseris, E. H. Sargent, F. Laquai and S. De Wolf, *Energy Environ. Sci.*, 2021, **14**, 4377.
69 K. Liu, S. Chen, J. Wu, H. Zhang, M. Qin, X. Lu, Y. Tu, Q. Meng and X. Zhan, *Energy Environ. Sci.*, 2018, **11**, 3463.
70 Z. Xing, F. Liu, S. H. Li, Z. C. Chen, M. W. An, S. Zheng, A. K. Y. Jen and S. Yang, *Adv. Funct. Mater.*, 2021, **31**, 2107695.
71 R. Zahran and Z. Hawash, *Adv. Mater. Interfaces*, 2022, **9**, 2201438.
72 G. Sathiyan, E. K. T. Sivakumar, R. Ganesamoorthy, R. Thangamuthu and P. Sakthivel, *Tetrahedron Lett.*, 2016, **57**, 243.
73 A. Jegorov, M. A. Truong, R. Murdey, M. Daskeviciene, T. Malinauskas, K. Kantminiene, V. Jankauskas, V. Getautis and A. Wakamiya, *Sol. RRL*, 2022, **6**, 2100877.
74 K. Radhakrishna, S. Beranagodu Manjunath, D. Devadiga, R. Chetri and A. Tantri Nagaraja, *ACS Appl. Energy Mater.*, 2023, **6**, 3635.
75 A. Magomedov, A. Al-Ashouri, E. Kasparavicius, S. Strazdaite, G. Niaura, M. Jošt, T. Malinauskas, S. Albrecht and V. Getautis, *Adv. Energy Mater.*, 2018, **8**, 1801892.
76 A. Al-Ashouri, A. Magomedov, M. Roß, M. Jošt, M. Talaikis, G. Chistiakova, T. Bertram, J. A. Márquez, E. Köhnen, E. Kasparavičius, S. Levcenco, L. Gil-Escrig, C. J. Hages, R. Schlatmann, B. Rech, T. Malinauskas, T. Unold, C. A. Kaufmann, L. Korte, G. Niaura, V. Getautis and S. Albrecht, *Energy Environ. Sci.*, 2019, **12**, 3356.
77 G. Kapil, T. Bessho, Y. Sanehira, S. R. Sahamir, M. Chen, A. Kumar Baranwal, D. Liu, Y. Sono, D. Hirotani, D. Nomura, K. Nishimura, M. Akmal Kamarudin, Q. Shen, H. Segawa and S. Hayase, *ACS Energy Lett.*, 2022, **7**, 966.
78 S. H. Hsiao, S. C. Peng, Y. R. Kung, C. M. Leu and T. M. Lee, *Eur. Polym. J.*, 2015, **73**, 50.
79 L. Li, Y. Wang, X. Wang, R. Lin, X. Luo, Z. Liu, K. Zhou, S. Xiong, Q. Bao, G. Chen, Y. Tian, Y. Deng, K. Xiao, J. Wu, M. I. Saidaminov, H. Lin, C. Q. Ma, Z. Zhao, Y. Wu, L. Zhang and H. Tan, *Nat. Energy*, 2022, **7**, 708.
80 R. Mishima, M. Hino, M. Kanematsu, K. Kishimoto, H. Ishibashi, K. Konishi, S. Okamoto, T. Irie, T. Fujimoto and W. Yoshida, *Appl. Phys. Express*, 2022, **15**, 076503.
81 Y. Lin, A. Magomedov, Y. Firdaus, D. Kaltsas, A. El-Labban, H. Faber, D. R. Naphade, E. Yengel, X. Zheng, E. Yarali, N. Chaturvedi, K. Loganathan, D. Gkeka, S. Alshammari, O. Bakr, F. Laquai, L. Tsetseris, V. Getautis and T. Anthopoulos, *ChemSusChem*, 2021, **14**, 3569.
82 Y. S. Shin, S. Ameen, E. Oleiki, J. Yeop, Y. Lee, S. Javaid, C. B. Park, T. Song, D. Yuk, H. Jang, Y. J. Yoon, W. Lee, G. Lee, B. Kim and J. Y. Kim, *Adv. Opt. Mater.*, 2022, **10**, 2201313.
83 A. Al-Ashouri, E. Köhnen, B. Li, A. Magomedov, H. Hempel, P. Caprioglio, J. A. Márquez, A. B. Morales Vilches, E. Kasparavicius, J. A. Smith, N. Phung, D. Menzel, M. Grischek, L. Kegelmann, D. Skroblin, C. Gollwitzer, T. Malinauskas, M. Jošt, G. Matič, B. Rech, R. Schlatmann, M. Topič, L. Korte, A. Abate, B. Stannowski, D. Neher, M. Stolterfoht, T. Unold, V. Getautis and S. Albrecht, *Science*, 2020, **370**, 1300.
84 X. Deng, F. Qi, F. Li, S. Wu, F. R. Lin, Z. Zhang, Z. Guan, Z. Yang, C. S. Lee and A. K.-Y. Jen, *Angew. Chem., Int. Ed.*, 2022, **61**, e202203088.
85 C. Rodríguez-Seco, M. Méndez, C. Roldán-Carmona, R. Pudi, M. K. Nazeeruddin and E. Palomares, *Angew. Chem.*, 2020, **132**, 5341.
86 E. Aktas, N. Phung, H. Kobler, D. A. González, M. Méndez, I. Kafedjiska, S. H. Turren-Cruz, R. Wenisch, I. Lauermann, A. Abate and E. Palomares, *Energy Environ. Sci.*, 2021, **14**, 3976.
87 S. Kumari, J. G. Sánchez, M. Imran, E. Aktas, D. A. González, L. Manna, E. Martínez-Ferrero and E. Palomares, *J. Mater. Chem. C*, 2023, **11**, 3788.

88 S. Zhang, R. Wu, C. Mu, Y. Wang, L. Han, Y. Wu and W. H. Zhu, *ACS Mater. Lett.*, 2022, **4**, 1976.
89 W. Jiang, F. Li, M. Li, F. Qi, F. R. Lin and A. K. Y. Jen, *Angew. Chem., Int. Ed.*, 2022, **61**, e202213560.
90 R. He, W. Wang, Z. Yi, F. Lang, C. Chen, J. Luo, J. Zhu, J. Thiesbrummel, S. Shah, K. Wei, Y. Luo, C. Wang, H. Lai, H. Huang, J. Zhou, B. Zou, X. Yin, S. Ren, X. Hao, L. Wu, J. Zhang, J. Zhang, M. Stolterfoht, F. Fu, W. Tang and D. Zhao, *Nature*, 2023, **618**, 80.
91 L. Calio, S. Kazim, M. Graetzel and S. Ahmad, *Angew. Chem., Int. Ed.*, 2016, **55**, 14522.
92 A. Farokhi, H. Shahroosvand, G. Delle Monache, M. Pilkington and M. Khaja Nazeeruddin, *Chem. Soc. Rev.*, 2022, **51**, 5974.
93 L. Nakka, Y. Cheng, A. Gerhard Aberle and F. Lin, *Adv. Energy Sustainability Res.*, 2022, **3**, 2200045.
94 Y. Wang, L. Duan, M. Zhang, Z. Hameiri, X. Liu, Y. Bai and X. Hao, *Sol. RRL*, 2022, **6**, 2200234.
95 E. Yalcin, D. A. Kara, C. Karakaya, M. Z. Yigit, A. K. Havare, M. Can, C. Tozlu, S. Demic, M. Kus and A. Aboulouard, *Opt. Mater.*, 2017, **69**, 283.
96 E. Yalcin, M. Can, C. Rodriguez-Seco, E. Aktas, R. Pudi, W. Cambarau, S. Demic and E. Palomares, *Energy Environ. Sci.*, 2019, **12**, 230.
97 E. Aktas, R. Pudi, N. Phung, R. Wenisch, L. Gregori, D. Meggiolaro, M. A. Flatken, F. De Angelis, I. Lauermann, A. Abate and E. Palomares, *ACS Appl. Mater. Interfaces*, 2022, **14**, 17461.
98 Y. Wang, Q. Liao, J. Chen, W. Huang, X. Zhuang, Y. Tang, B. Li, X. Yao, X. Feng, X. Zhang, M. Su, Z. He, T. J. Marks, A. Facchetti and X. Guo, *J. Am. Chem. Soc.*, 2020, **142**, 16632.
99 Q. Liao, Y. Wang, Z. Zhang, K. Yang, Y. Shi, K. Feng, B. Li, J. Huang, P. Gao and X. Guo, *J. Energy Chem.*, 2022, **68**, 87.
100 R. Guo, X. Zhang, X. Zheng, L. Li, M. Li, Y. Zhao, S. Zhang, L. Luo, S. You, W. Li, Z. Gong, R. Huang, Y. Cui, Y. Rong, H. Zeng and X. Li, *Adv. Funct. Mater.*, 2023, **33**, 2211955.
101 H. Liu, K. Yan, J. Rao, Z. Chen, B. Niu, Y. Huang, H. Ju, B. Yan, J. Yao, H. Zhu, H. Chen and C. Z. Li, *ACS Appl. Mater. Interfaces*, 2022, **14**, 6794.
102 L. Mao, Y. Wu, J. Jiang, X. Guo, P. Heng, L. Wang and J. Zhang, *J. Phys. Chem. C*, 2020, **124**, 9233.
103 S. Thokala and S. P. Singh, *ACS Omega*, 2020, **5**, 5608.
104 G. D. Blanco, A. J. Hiltunen, G. N. Lim, C. B. KC, K. M. Kaunisto, T. K. Vuorinen, V. N. Nesterov, H. J. Lemmetyinen and F. D'Souza, *ACS Appl. Mater. Interfaces*, 2016, **8**, 8481.
105 E. Li, E. Bi, Y. Wu, W. Zhang, L. Li, H. Chen, L. Han, H. Tian and W. H. Zhu, *Adv. Funct. Mater.*, 2019, **30**, 1909509.
106 E. Li, C. Liu, H. Lin, X. Xu, S. Liu, S. Zhang, M. Yu, X. M. Cao, Y. Wu and W. H. Zhu, *Adv. Funct. Mater.*, 2021, **31**, 2103847.
107 A. Ullah, K. H. Park, H. D. Nguyen, Y. Siddique, S. F. A. Shah, H. Tran, S. Park, S. I. Lee, K. K. Lee, C. H. Han, K. Kim, S. Ahn, I. Jeong, Y. S. Park and S. Hong, *Adv. Energy Mater.*, 2021, **32**, 2103175.
108 A. Ullah, K. H. Park, Y. W. Lee, S. Park, A. Bin Faheem, H. D. Nguyen, Y. Siddique, K. K. Lee, Y. Jo, C. H. Han, S. Ahn, I. Jeong, S. Cho, B. Kim, Y. S. Park and S. Hong, *Adv. Funct. Mater.*, 2022, **32**, 2208793.
109 S. Liu, W. Cao, D. Xia, J. Zhang, J. Fan, C. An, R. Fan, S. Hao, K. Lin and Y. Yang, *Dyes Pigm.*, 2021, **193**, 109506.
110 E. Arkan, E. Yalcin, M. Unal, M. Zeliha Yigit Arkan, M. Can, C. Tozlu and S. Demic, *Mater. Chem. Phys.*, 2020, **254**, 123435.
111 E. Arkan, M. Unal, E. Yalcin, M. Zeliha Yigit Arkan, S. Yurtdas, M. Can, C. Tozlu and S. Demic, *Mater. Sci. Semicond. Process.*, 2021, **123**, 105514.
112 E. Arkan, M. Zeliha Yigit Arkan, M. Unal, E. Yalcin, H. Aydin, C. Celebi, M. Can, C. Tozlu and S. Demic, *Opt. Mater.*, 2020, **105**, 109910.
113 C. Zhang, W. Kong, T. Wu, X. Lin, Y. Wu, J. Nakazaki, H. Segawa, X. Yang, Y. Zhang, Y. Wang and L. Han, *ACS Appl. Mater. Interfaces*, 2021, **13**, 44321.
114 L. Li, Y. Wu, E. Li, C. Shen, H. Zhang, X. Xu, G. Wu, M. Cai and W. H. Zhu, *Chem. Commun.*, 2019, **55**, 13239.
115 H. Cheng, Y. Li, M. Zhang, K. Zhao and Z. S. Wang, *ChemSusChem*, 2020, **13**, 2779.
116 E. Aktas, J. Jiménez-López, K. Azizi, T. Torres and E. Palomares, *Nanoscale Horiz.*, 2020, **5**, 1415.
117 H. Kouki, S. Pitié, A. Torkhani, F. Mamèche, P. Decorse, M. Seydou, F. Kouki and P. Lang, *ACS Appl. Energy Mater.*, 2022, **5**, 1635.
118 M. A. Truong, T. Funasaki, L. Ueberricke, W. Nojo, R. Murdey, T. Yamada, S. Hu, A. Akatsuka, N. Sekiguchi, S. Hira, L. Xie, T. Nakamura, N. Shioya, D. Kan, Y. Tsuji, S. Iikubo, H. Yoshida, Y. Shimakawa, T. Hasegawa, Y. Kanemitsu, T. Suzuki and A. Wakamiya, *J. Am. Chem. Soc.*, 2023, **145**, 7528.
119 S. N. Afraj, C. H. Kuan, J. S. Lin, J. S. Ni, A. Velusamy, M. C. Chen and E. W. G. Diau, *Adv. Funct. Mater.*, 2023, **33**, 2213939.
120 W. Li, M. Cariello, M. Méndez, G. Cooke and E. Palomares, *ACS Appl. Energy Mater.*, 2023, **6**, 1239.

